ISSN: 2165-3259

JAOCR

Official Journal of the American Osteopathic College of Radiology

EMERGENCY RADIOLOGY

Guest Editor: Hemang Kotecha, D.O.

Editor-in-Chief: Daniel J. Wale, D.O.

April 2020, Vol. 9, Issue 2

JAOCR

Official Journal of the American Osteopathic College of Radiology

Aims and Scope

The Journal of the American Osteopathic College of Radiology (JAOCR) is designed to provide practical up-to-date reviews of critical topics in radiology for practicing radiologists and radiology trainees. Each quarterly issue covers a particular radiology subspecialty and is composed of high-quality review articles and case reports that highlight differential diagnoses and important teaching points.

Access to Articles

All articles published in the JAOCR are open access online. Subscriptions to the journal are not required to view or download articles. Reprints are not available.

Copyrights

Guide for Authors

Submissions for the JAOCR are by invitation only. If you were invited to submit an article and have questions regarding the content or format, please contact the appropriate Guest Editor for that particular issue. Although contributions are invited, they are subject to peer review and final acceptance.

Editor-in-Chief

Editor Emeritus

Editorial Board

JAOCR

EMERGENCY RADIOLOGY

Guest Editor: Hemang Kotecha, D.O.

From the Editor

Review Articles

Differential-Based Case Reviews

JAOCR at the Viewbox

In this Issue

Hemang Kotecha, D.O.

"Above all, don't fear difficult moments. The best comes from them."

Rita Levi-Montalcini

Hemang Kotecha, D.O.

Assistant Professor, University of Massachusetts, Worcester, MA
UMass Memorial Medical Center, Worcester, MA

I am frequently met with confused expressions when I tell other physicians, including radiologists, that I am an emergency radiologist. Most people are not aware that such a subspecialty exists within radiology, and almost all inquire as to what the profession entails.

The field of emergency radiology initially emerged to meet demands for 24/7 diagnostic radiology coverage and has grown as imaging utilization has skyrocketed in emergency departments, both in academic and private practices. Our academic institution covers five emergency departments, including a level 1 trauma and comprehensive stroke center, and emergency radiologists provide final reports on all imaging studies 24 hours a day, 7 days a week, 365 days a year. Our residents and fellows are trained in emergency pathology, department-specific imaging workflow, best protocols and practices, utilization of advanced imaging techniques including dual-energy CT and rapid protocol MRI, as well as incorporating artificial intelligence into daily practice. We work closely with emergency medicine physicians and acute-care/trauma surgeons to care for adult and pediatric patients with both traumatic and nontraumatic acute illnesses, with an emphasis on rapid, comprehensive, and accurate diagnoses. This includes stroke, head and neck, thoracic, vascular, gastrointestinal, genitourinary, musculoskeletal, and head to toe trauma imaging utilizing conventional radiography, CT, MRI, ultrasound, fluoroscopy, and nuclear medicine.

In this emergency radiology issue of the JAOCR, our goal was to complement the recent issue on trauma imaging by highlighting several stimulating nontrauma topics encountered in emergency radiology. Our review articles emphasize common oncologic emergencies in the abdomen and pelvis and lay the foundation for approaching neck infections — two daunting conditions encountered in the emergency department. Our case reviews and Viewbox articles feature a variety of musculoskeletal, vascular, gastrointestinal, and pulmonary conditions that may cause diagnostic dilemmas for radiologists.

I am privileged to serve as guest editor for this issue, and I would like to thank my mentor and colleague Christopher Cerniglia, D.O., for nominating me for this role, and Daniel Wale, D.O., for his guidance and support throughout this project. Residents from our program were heavily involved in each article, and I am indebted to all our department faculty for their mentorship. We hope these articles will both educate our readership on the selected clinical subjects and provide a glimpse into the scope of emergency radiology.

Neck Infections: What the Radiologist Needs to Know

Roberto Kutcher-Diaz, M.D., David Radcliffe, M.D., Hao Lo, M.D., Hemang Kotecha, D.O., Gabriela Santos-Nunez, M.D.

Department of Radiology, UMass Memorial Medical Center, Worcester, MA

Neck infections represent common clinical emergencies. While diagnosis and treatments are often merely clinical, approximately 10% to 20% of deep neck infection complications are potentially life threatening.[1] Common etiologies for head and neck infection include pharyngitis, mastoiditis, and odontogenic infections. Localization and patterns of spread, especially involving the deep cervical spaces, can be challenging for the treating clinician. Clinical manifestations vary based on the age of presentation and infection site. CT of the neck is the first line of imaging in the acute setting.[2] Although anatomy of the head and neck is challenging, knowledge of common imaging patterns and complications is critical for prompt and accurate diagnosis, which will minimize adverse outcomes.[1]

Cervical Fascia

While there is considerable variation in the description of the cervical fascial layers, a commonly utilized classification system is based on topographic morphology and distinguishes between the superficial and deep fascia, with the deep fascia being further classified into the superficial, middle, and deep layers. The superficial fascia is of limited clinical importance to radiologists as it is a connective layer interposed between the skin and deep fascia. By comparison, the deep fascia is significant to radiologists as understanding fascial boundaries allows for easier detection of disease, more refined differential diagnoses, anticipated routes of disease spread and subsequent complications.[3,4]

The first layer of the deep cervical fascia, the superficial layer, is also known as the investing layer. The superficial layer of the deep cervical fascia (SLDCF) encircles the neck with attachment to the spinous processes and ligamentum nuchae posteriorly; hyoid bone anteriorly; the mandible, temporal, and occipital bones superiorly; and the manubrium, clavicles, and scapulae inferiorly. Through its course, the external layer encompasses the stylohyoid and digastric muscles at the level of the suprahyoid neck; the parotid glands superiorly; the sternocleidomastoid muscles anteriorly; and the trapezius muscles posteriorly. The SLDCF is also continuous with the pectoralis major fascia as well as the trapezius and latissimus dorsi fascia.[3,4]

The middle layer, also known as the pretracheal layer, can be further broken down into the muscular and visceral divisions. The muscular division encircles the infrahyoid, geniohyoid, and mylohyoid muscles with superior attachment to the hyoid and thyroid cartilage and inferior continuity with the clavipectoral fascia. The visceral division of the pretracheal layer encircles the thyroid, parathyroid glands, trachea, and esophagus. The posterior aspect of the visceral division, also named the buccopharyngeal fascia, extends from the skull base to the thoracic cavity where it attaches to the pericardium. This layer is of particular clinical significance given that the retropharyngeal spaces lies directly posterior to the buccopharyngeal fascia.[3,4]

The deep layer of the deep cervical fascia (DLDCF), also known as the prevertebral fascia, attaches to the ligamentum nuchae posteriorly, encircles the paraspinal musculature, attaches to the transverse processes, encircles the prevertebral musculature, and extends anteriorly where it lies immediately posterior to the buccopharyngeal fascia. Superiorly, the DLDCF attaches to the skull base. Inferiorly, DLDCF is contiguous with the anterior longitudinal ligament, contributes to the transversalis fascia, axillary sheath, and Sibson's fascia. Of note, the carotid sheath is considered by some to be included as a portion of the deep fascia, while other sources

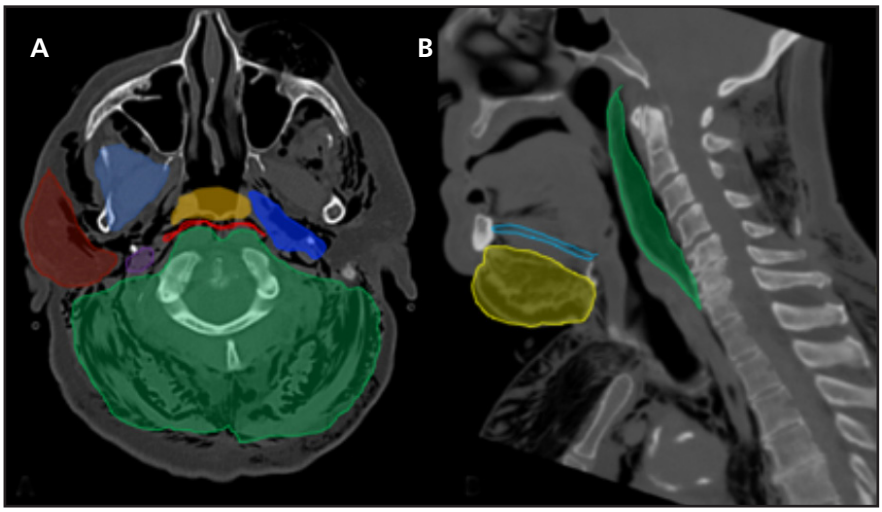

FIGURE 1. *Axial (A) and sagittal (B) CT images in a patient with subcutaneous emphysema delineating the anatomical compartments of the neck. In (A), purple color encircles poststyloid (retrostyloid) parapharyngeal space. Navy blue denotes the parapharyngeal space. Red delineates the retropharyngeal space. Mustard yellow encloses the pharyngeal mucosal space. Light blue outlines the masticator space. Green denotes the posterior cervical compartment, including the prevertebral space. Maroon demonstrates the parotid space. In (B), yellow encircles the submandibular space. Light blue outlines the sublingual space. Green denotes the prevertebral space*

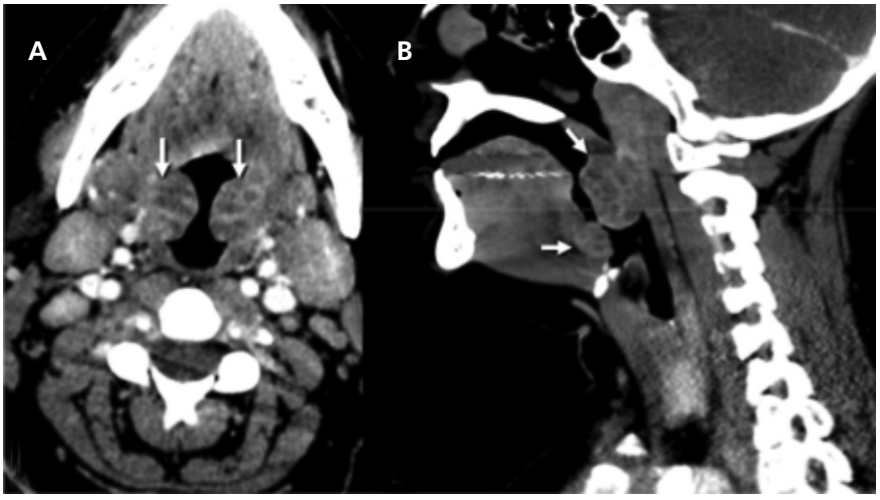

FIGURE 2. *Tonsillitis. Axial (A) and coronal (B) contrast-enhanced CT images of the neck at the level of the oropharynx. Striated-appearing palatine tonsils (arrows in A) and lingual tonsils (arrows in B) are typical of streptococcal infection.*

consider it a separate entity composed of portions of the external, middle, and deep fascial layers.[3,4]

Parapharyngeal Space

The parapharyngeal space (PPS) is a paired region extending from the skull base to the hyoid bone. From its anterior edge at the pterygomandibular raphe, the lateral border demarcated by SLDCF extends dorsally medial to the masticator space and deep portion of the parotid gland. The posterior margins are defined by the deep layer of the deep cervical fascia DLDCF at the dorsal aspect of the carotid sheath. Several fascial layers within the space define up to three compartments with varying degrees of communication. These compartments are grouped by some authors as prestyloid and poststyloid parapharyngeal spaces, which others term the *parapharyngeal space* and *carotid space*, respectively. The former contains fat and minor salivary glands, while the latter contains the internal carotid artery (ICA), internal jugular vein, and cranial nerves IX-XII. In the suprahyoid neck, as opposed to infrahyoid, most authors consider the carotid sheath to be an incomplete structure. At the level of the angle of the mandible and ICA, the carotid space is invested by the same fascial layers as the parapharyngeal space, thus becoming a posterior (retrostyloid) compartment of the latter (**Figure 1**).[5]

Parapharyngeal Infections

PPS is largely constituted by fat; therefore, pathology arising from the space is relatively uncommon. Its importance relies on multiple anatomic relationships. The PPS serves to corroborate where pathology originates. Adjacent lesions will shift the PPS in different directions.[6] PPS infections typically occur via the palatine tonsil or by spreading from odontogenic, paranasal sinuses, and parotid gland infections.[2] The lymphatic drainage of these structures leads to lymph nodes in the retropharyngeal and PPS.[7]

Pharyngeal Mucosal Space and Peritonsillar Space

Pharyngeal mucosal space contains both mucosal and lymphoid tissue. The peritonsillar space is a continuation of the pharyngeal mucosal space, which is divided into nasopharyngeal, oropharyngeal, and hypopharyngeal segments. It is bordered by the deep cervical fascia middle layer along the lateral and posterior margins. It is not, however, a true enclosed fascial space because no fascia is present along the airway surface. The retropharyngeal space is located directly posterior, while the parapharyngeal space lies laterally. The intrinsic contents include pharyngeal mucosa, lymphatic ring (adenoids, palatine tonsils, lingual tonsils), minor salivary glands, torus tubarius (pharyngeal end of the eustachian tube), and pharyngeal musculature (superior and middle constrictor, salpingopharyngeus, levator palatini).[6,8]

Pharyngeal Mucosal Infections

Many aerodigestive tract infections start in the pharyngeal mucosal space. Infections in this space can demonstrate

FIGURE 3. *Peritonsillar abscess. Axial contrast-enhanced CT of the neck shows an ill-defined region of necrosis centered in the left peritonsillar region (arrows). Local mass effect results in narrowing of oropharyngeal airway.*

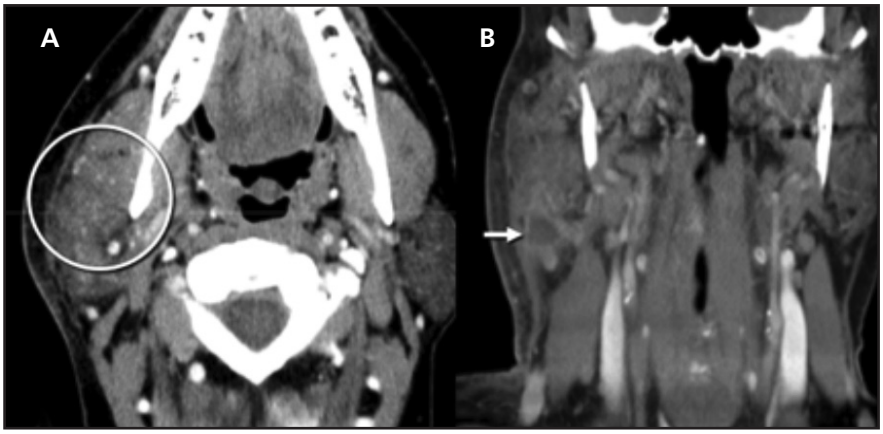

FIGURE 4. *Sialadenitis. Axial image (A) from contrast-enhanced neck CT demonstrates an enlarged enhancing right parotid gland (circle) with surrounding fat stranding and thickening of the platysma. An intraglandular rim-enhancing collection in the lower pole of the superficial lobe (arrow in B) indicates an abscess.*

FIGURE 5. *Calculus sialadenitis. Axial contrast-enhanced CT neck at the level of the right submandibular space demonstrates a sialolith (arrow) in a dilated right submandibular duct. The submandibular gland (arrowhead) is enlarged and enhancing.*

a wide array of signs and symptoms including pharyngitis, tonsillitis, suppuration, and tonsillar abscess.[1] In general, these are polymicrobial infections with diverse aerobic and anaerobic flora. Nonetheless, *Fusobacterium necrophorum* and Streptococcus group A are among the most prevalent pathogens.[9] Tonsillitis is a clinical diagnosis, but as inflammation progresses, suppuration and phlegmon can develop. Imaging findings consist of diffusely enlarged tonsils, abscess formation, and peritonsillar inflammation (**Figure 2**). Tonsillar abscess typically originates between the tonsillar capsule and pillar (**Figure 3**). Distinction between phlegmon and abscess is important as it will dictate clinical management. If an abscess is present, aspiration is the standard of care.[10]

Submandibular/Sublingual Space

The submandibular space corresponds to the compartment at the floor of the mouth (**Figure 1**). Contiguous across the midline ventrally, it is outlined anteriorly by the arch of the mandible and posteriorly by the submandibular glands. Its superior margin, the mucosa of the floor of the mouth, can be appreciated on physical examination. Caudally it is bounded by insertion of the SLDCF into the hyoid bone. The space is subdivided into two compartments by the mylohyoid muscle: the sublingual (superiorly) and submandibular (inferiorly). The sublingual compartment contains the sublingual glands, the duct and deep portion of the submandibular gland, the lingual vessels, and the glossal/hypoglossal nerves. The submaxillary space contains the superficial portion of the submandibular gland. The compartments communicate at the posterior margin of the mylohyoid, which accounts for the "diving" appearance of a ruptured ranula. In 77% of cases, the compartments may communicate through a defect in the mylohyoid muscle (a boutonniere), which may present as a palpable lump of a herniated sublingual gland.[5,11]

Parotid Space

The parotid space (PS) contains the parotid gland, which is bifurcated by the facial nerve into superficial and deep lobes. On routine CT or MRI, a more conspicuous anatomic landmark is the retromandibular vein, which lies just medial to the facial nerve. Another landmark is the external carotid artery, located immediately medial to the retromandibular vein. The SLDCF surrounds the parotid space (**Figure 1**). Craniocaudally, the parotid space extends from the external auditory canal/mastoid tip to the parotid tail, just below the mandibular angle. The parotid tail lies between the platysma and sternocleidomastoid muscles. The poststyloid (retrostyloid) parapharyngeal space is posteromedial to the parotid space, separated by the digastric muscle posterior belly. The parapharyngeal space lies medial to the parotid space. The contents of the parotid space include the parotid gland, facial nerve, retromandibular vein, external carotid artery branches, lymph nodes, and parotid (Stensen) ducts.[8]

A common anatomic variant is the parotid gland accessory third lobe, superficial to the masseter muscle. The parotid duct courses along the margin of the masseter muscle, entering the buccinator

FIGURE 6. *Suppurative retropharyngeal lymphadenopathy. Axial contrast-enhanced CT of the neck at the level of the oropharynx demonstrates an enlarged left retropharyngeal lymph node (also known as node of Rouviere), with central necrosis (circle).*

muscle at the level of the second maxillary molar. A normal duct is too small for routine identification on imaging. Intraparotid lymph nodes are routinely seen because parotid gland encapsulation occurs after nodal chain development.[6]

Salivary Gland Infections

Acute sialadenitis may be viral, bacterial or calculus induced. Patients are typically ill with acute pain exacerbated by food. Leukocytosis is usually present.[1,2] When dealing with salivary gland infections it is fundamental to consider symptom chronicity and laterality. This approach will help the interpreting radiologist distinguish between isolated and systemic pathologies and will also aid in selecting the imaging modality of choice. For example, a sialolith may be better depicted by CT than MRI. Bacterial infections are more common in adults following recent surgery with intubation and dehydration as predisposing factors (**Figure 4**). *Staphylococcus aureus* is amongst common pathogens in adults, whereas Paramyxovirus (mumps) is the most common culprit in the pediatric population, but other viruses such as adenovirus and parainfluenza are also common pathogens. When multiple lesions are within the parotid gland, HIV infection should also be considered as a possible diagnosis.[12]

Imaging will demonstrate an enlarged gland with periglandular inflammatory change. A dilated duct may be present in cases of calculus sialadenitis (**Figure 5**). Chronic sialadenitis may present with a firm and painless gland with fatty atrophy. Abscess formation constitutes a late complication with the parotid gland being the most common location. Viral sialadenitis is a systemic process, usually bilateral, and may involve more than one group of salivary glands.[2]

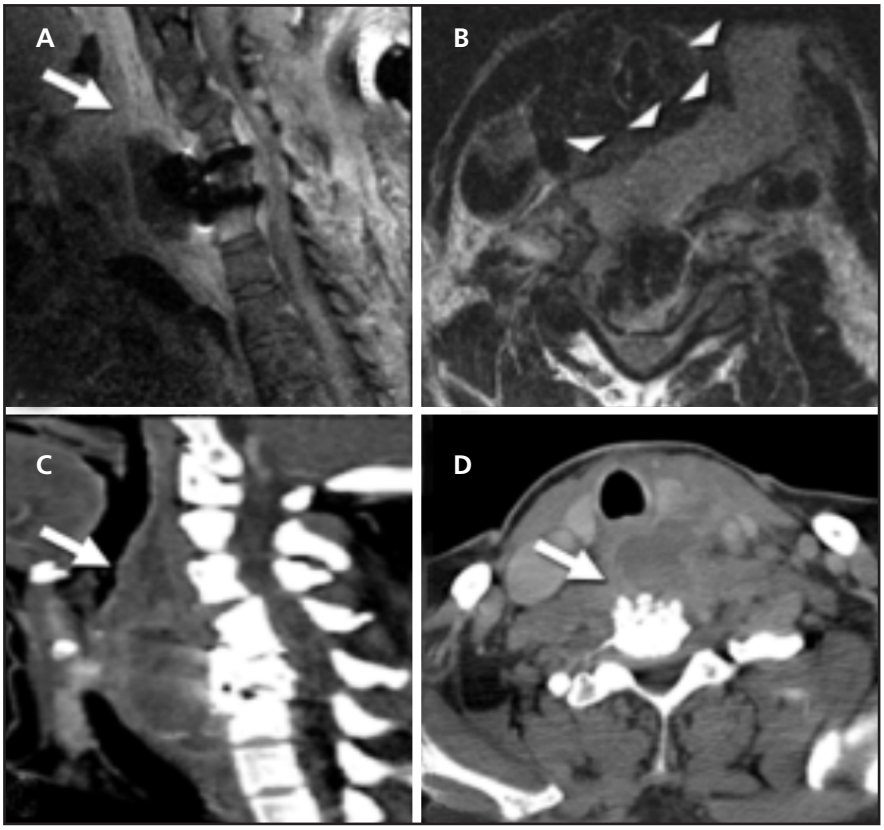

FIGURE 7. *Prevertebral abscess. Sagittal T1 postcontrast (A) and axial T2-weighted (B) images of the cervical spine in a patient with anterior corpectomy/discectomy and instrumented fusion demonstrate enhancement of prevertebral soft tissues (arrows in A) and a large abscess in the surgical bed (arrowheads in B). Axial (C) and sagittal (D) CT images in the same patient also demonstrate the abscess (arrows) in the surgical bed.*

Retropharyngeal (Retrovisceral) Space

The retropharyngeal or retrovisceral space (RS) spans the suprahyoid and infrahyoid neck as contiguous retropharyngeal and retroesophageal spaces (**Figure 1**). The region extends from the skull base caudally to the mediastinal fusion of the anterior buccopharyngeal and posterior alar fascia (most commonly near the level of the tracheal bifurcation). Laterally, a band of fascia known as the *cloison sagittale* separates it from the parapharyngeal space. The RS and pretracheal spaces communicate around the esophagus between the thyroid cartilage and inferior thyroidal artery.[5,12]

Retropharyngeal Infections

Retropharyngeal infections constitute a deep neck infection allowing for potentially lethal complications. The suprahyoid RS contains lymph nodes and fat, whereas the infrahyoid RS only contains fat. Infections are secondary to direct spread or from direct inoculation in the setting of penetrating trauma. Patients can present with different symptoms depending on where the process arises. Infections usually begin in the pharynx, paranasal sinuses, middle ear, or prevertebral space. Contrast-enhanced CT of the neck is usually the imaging modality of choice. Findings vary from low

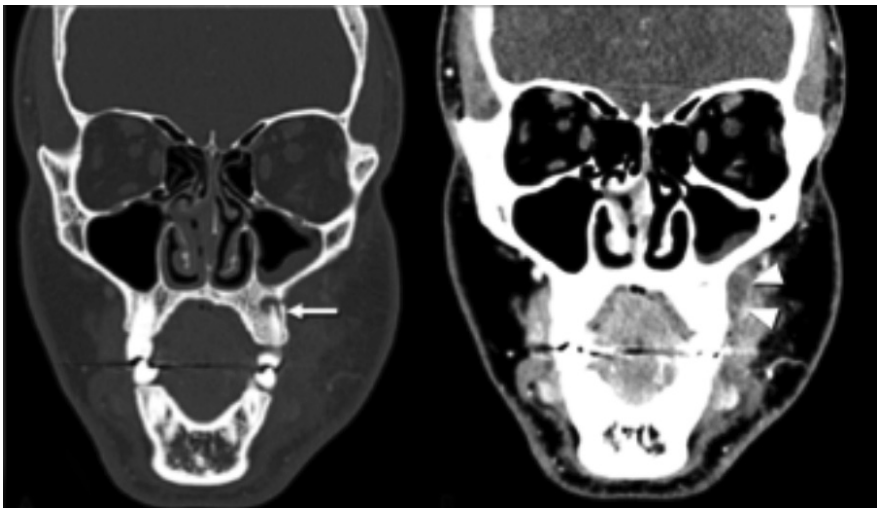

FIGURE 8. *Masticator space abscess. Contrast-enhanced coronal maxillofacial CT images in bone (A) and soft tissue (B) windows demonstrate a periapical lucency (arrow in A) surrounding a left maxillary molar tooth and dehiscence of the maxillary buccal cortex. An adjacent peripherally enhancing collection (arrowheads in B) represents a subperiosteal abscess.*

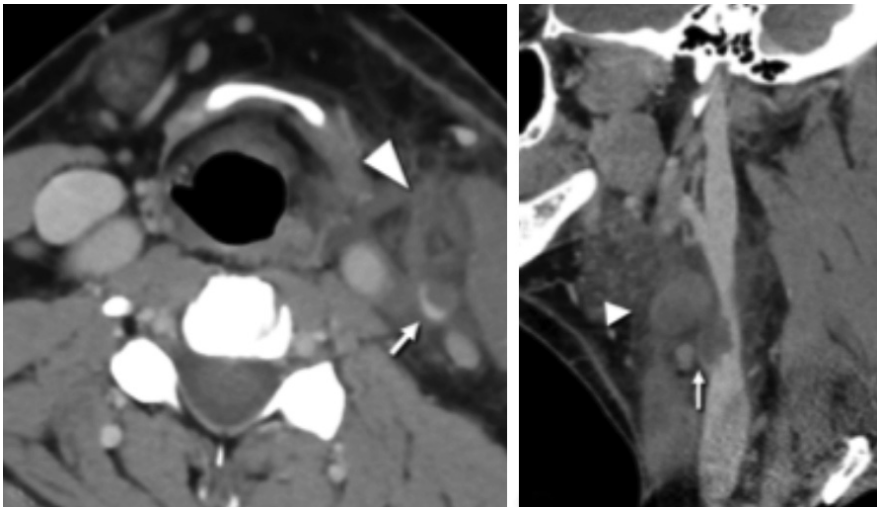

FIGURE 9. *Lemierre syndrome. Axial (A) and sagittal (B) contrast-enhanced CT of the neck demonstrates a nonocclusive filling defect within the left internal jugular vein (arrows) with surrounding fat stranding. Level III cervical lymphadenopathy (arrowhead) is also present anterior to the internal jugular vein.*

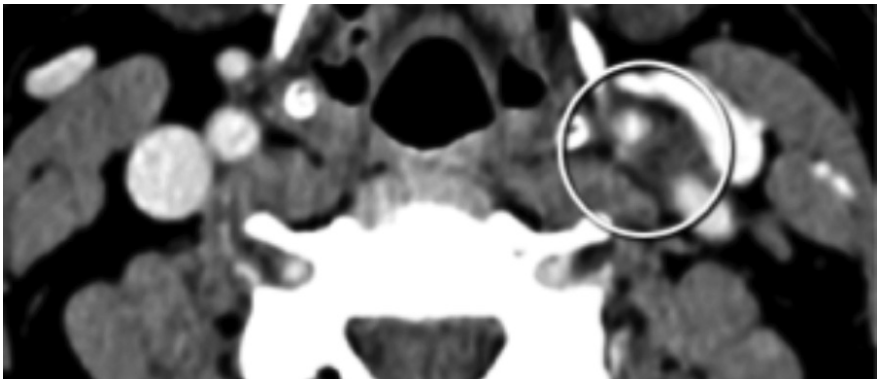

FIGURE 10. *Carotidynia. Axial image from contrast-enhanced CT angiogram of the neck at the carotid bifurcation shows circumferential soft-tissue thickening encasing and narrowing the left carotid bulb (circle).*

attenuation effusion of the RS to phlegmon and abscess formation. Impaired lymphoid drainage or excess lymphoid production will lead to local edema and nodal enlargement. Suppurative nodes and retropharyngeal abscess are at times used interchangeably. However, distinction between the two is important because it will dictate clinical management. Suppurative nodes consist of enlarged nodes with internal necrosis, with pus formation contained within the thick enhancing node capsule (**Figure 6**).[13,14] A retropharyngeal abscess usually manifests as a low attenuation fluid collection that will result in anterior displacement of the of the posterior pharyngeal wall from the prevertebral muscles. Retropharyngeal abscess does not typically exhibit a thick enhancing wall.[15]

Posterior Cervical Space

The posterior cervical space corresponds to the posterior triangle of the neck outlined by the sternocleidomastoid anteriorly and the trapezius posteriorly. The medial fascial boundary is demarcated by the DLDCF as it curves around the paraspinal muscles of the prevertebral space from the spinous processes/nuchal ligaments posteriorly, to the transverse processes of the cervical vertebra anteriorly (**Figure 1**). Although separate from this compartment, the posterior triangle also encompasses a space containing the spinal accessory nerve and its lymph node chain. Lymphadenopathy in this chain will result in a characteristic anterior displacement of the carotid sheath, which lies ventrally.

Pre- and Perivertebral Infections

The bulk of the pre- and perivertebral space (PVS) is comprised of muscles and osseous structures. Infection is common and usually occurs from direct inoculation after trauma or surgery, direct extension, or hematogenous spread. Predisposing risk factors include intravenous drug use and immunocompromised status. Symptoms vary, including neck pain, focal tenderness, and myelopathy if epidural involvement is present. *Staphylococcus aureus* is one

of the most commonly isolated pathogens. Contrast-enhanced CT and MRI are complementary when evaluating the PVS. Imaging findings include pre- or perivertebral fluid, myositis, endplate destruction (discitis/osteomyelitis and presence of hardware construct). Edema in this space will displace the longus capiti muscles, a helpful clue that will differentiate from a process arising in the RS (**Figure 7**). The DLDCF confines the infection so that it preferentially extends into the epidural space.[16,17] Nodal involvement is common.[14]

Masticator Space

The masticator space (MS) consists of paired spaces on each side of the face and is bounded by the SLDCF. The SLDCF splits in two layers at the lower border of the mandible. The superficial layer encloses the masseter muscle extending over the zygomatic arch and attaches to the lateral orbital wall. The deep layer extends medial to the medial pterygoid muscle and attaches to the skull base medial to the foramen ovale. These two layers fuse along the borders of the mandibular ramus.[5,15] The MS comprises masticator muscles (pterygoid, masseter and temporalis) and the posterior mandibular ramus.[19]

Masticator Infections

Clinical evaluation of the masticator space is limited. Patients may complain of trismus mimicking temporomandibular joint disease. Most MS infections are the result of direct spread of advanced odontogenic infections (**Figure 8**). Several pathways of spread had been proposed, which include a cortical break along the buccal aspect of the maxillary bone with propagation along the medial pterygoid muscle fibers. Secondary extension is directed superiorly along interlaced muscle fibers and vertical orientation of the cervical fascia.[20] Imaging findings include edema and muscle stranding with occasionally phlegmon/abscess formation, classically situated adjacent to the mandibular ramus.[2]

Unique Entities

Lemierre Syndrome

Acute oropharyngeal infection can cause septic thrombophlebitis of the internal jugular vein. This process is almost exclusively caused by *Fusobacterium necrophorum*. Infection occurs after lateral spread from the lateral pharyngeal space. Neck swelling and tenderness are the hallmark symptoms (**Figure 9**). Pulmonary nodules are also found as the venous system serves as a route of metastatic spread. Contrast-enhanced CT of the neck is the modality of choice and will demonstrate thrombosis of the internal jugular vein and thrombophlebitis.[2]

Carotidynia or Fay Syndrome

This is a poorly understood syndrome manifested by unilateral neck pain and increased pulsation in the affected side.[21] Imaging findings consist of amorphous soft tissue or stranding replacing the fat surrounding the carotid artery without luminal narrowing. Patients usually complain of neck pain with tenderness to palpation over the carotid bifurcation (**Figure 10**).[22]

Summary

Imaging plays an important role in the evaluation of neck infections and CT and/or MR imaging is commonly obtained in the emergency department. Clinical presentations vary based upon the neck compartment in which each entity arises. Knowledge of the imaging patterns and potential complications of various infectious processes will allow the radiologist to provide an accurate and prompt diagnosis, evaluate for potential complications, and ensure optimal treatment.

References

1. Kubal WS. Face and neck infections: what the emergency radiologist needs to know. Radiol Clin North Am 2015;53(4):827-846. doi:10.1016/j.rcl.2015.02.007
2. Maroldi R, Farina D, Ravanelli M, Lombardi D, Nicolai P. Emergency imaging assessment of deep neck space infections. Semin Ultrasound CT and MRI 2012;33(5):432-442. doi:10.1053/j.sult.2012.06.008
3. King KM. Head and neck imaging. 3rd ed, 2 vols. Radiology 1997;204(1):220-220. doi:10.1148/radiology.204.1.220
4. Sutcliffe P, Lasrado S. Anatomy, head and neck, deep cervical neck facia. In: StatPearls. StatPearls Publishing; 2019. http://www.ncbi.nlm.nih.gov/books/NBK541091/. Accessed December 6, 2019.
5. Guidera AK, Dawes PJD, Fong A, Stringer MD. Head and neck fascia and compartments: no space for spaces. Head Neck 2014;36(7):1058-1068. doi:10.1002/hed.23442
6. Gamss C, Gupta A, Chazen JL, Phillips CD. Imaging evaluation of the suprahyoid neck. Radiol Clin North Am 2015;53(1):133-144. doi:10.1016/j.rcl.2014.09.009
7. Weber AL, Siciliano A. CT and MR imaging evaluation of neck infections with clinical correlations. Radiol Clin North Am 2000;38(5):941-968. doi:10.1016/S0033-8389(05)70214-1
8. Rubin JA, Wesolowski JR. Neck MR imaging anatomy. Magn Reson Imaging Clin N Am 2011;19(3):457-473, vii. doi:10.1016/j.mric.2011.05.003
9. Klug TE, Henriksen J-J, Fuursted K, Ovesen T. Significant pathogens in peritonsillar abscesses. Eur J Clin Microbiol Infect Dis 2011;30(5):619-627. doi:10.1007/s10096-010-1130-9
10. Ludwig BJ, Foster BR, Saito N, Nadgir RN, Castro-Aragon I, Sakai O. Diagnostic imaging in nontraumatic pediatric head and neck emergencies. RadioGraphics 2010;30(3):781-799. doi:10.1148/rg.303095156
11. La'Porte SJ, Juttla JK, Lingam RK. Imaging the floor of the mouth and the sublingual space. RadioGraphics. 2011;31(5):1215-1230. doi:10.1148/rg.315105062
12. Parker GD, Harnsberger HR. Radiologic evaluation of the normal and diseased posterior cervical space. Am J Roentgenol 1991;157(1):161-165. doi:10.2214/ajr.157.1.2048512
13. Shefelbine SE, Mancuso AA, Gajewski BJ, Ojiri H, Stringer S, Sedwick JD. Pediatric retropharyngeal lymphadenitis: differentiation from retropharyngeal abscess and treatment implications. Otolaryngol Head Neck Surg 2007;136(2):182-188. doi:10.1016/j.otohns.2006.03.002
14. Hoang JK, Branstetter BF, Eastwood JD, Glastonbury CM. Multiplanar CT and MRI of collections in the retropharyngeal space: is it an abscess? Am J Roentgenol 2011;196(4):W426-432. doi:10.2214/AJR.10.5116
15. Bou-Assaly W, Mckellop J, Mukherji S. Computed tomography imaging of acute neck inflammatory processes. World J Radiol 2010;2(3):91-96. doi:10.4329/wjr.v2.i3.91
16. Mills MK, Shah LM. Imaging of the perivertebral space. Radiol Clin North Am 2015;53(1):163-180. doi:10.1016/j.rcl.2014.09.008
17. Capps EF, Kinsella JJ, Gupta M, Bhatki AM, Opatowsky MJ. Emergency imaging assessment of acute, nontraumatic conditions of the head and neck. RadioGraphics 2010;30(5):1335-1352. doi:10.1148/rg.305105040
18. Wei Y, Xiao J, Zou L. Masticator space: CT and MRI of secondary tumor spread. Am J Roentgenol 2007;189(2):488-497.
19. Fernandes T, Lobo JC, Castro R, Oliveira MI, Som PM. Anatomy and pathology of the masticator space. Insights Imaging 2013;4(5):605-616. doi:10.1007/s13244-013-0266-4
20. Schuknecht B, Stergiou G, Graetz K. Masticator space abscess derived from odontogenic infection: imaging manifestation and pathways of extension depicted by CT and MR in 30 patients. Eur Radiol 2008;18(9):1972-1979. doi:10.1007/s00330-008-0946-5
21. Santarosa C, Stefanelli S, Sztajzel R, Mundada P, Becker M. Carotidynia: a rare diagnosis for unilateral neck pain revealed by cross-sectional imaging. Case Rep Radiol 2017;2017. doi:10.1155/2017/7086854
22. Lecler A, Obadia M, Savatovsky J, et al. TIPIC Syndrome: beyond the myth of carotidynia, a new distinct unclassified entity. Am J Neuroradiol 2017;38(7):1391-1398. doi:10.3174/ajnr.A5214

Oncologic Emergencies of the Abdomen and Pelvis

Evan Ruppell, D.O., Hemang Kotecha, D.O., Lacey McIntosh, D.O.

Department of Radiology, UMass Memorial Medical Center, Worcester, MA

Many of the more lethal malignancies originate from viscera in the abdomen and pelvis including tumors of the prostate, pancreas, liver, and colon/rectum.[1] In the ongoing work to improve patient survival, imagers must be cognizant of oncologic emergencies. These are defined as acute, potentially life-threatening events that develop as effects of cancer or its treatment. The most common oncologic emergencies relate to the gastrointestinal system and have a high association with mortality.[2,3] Oncologic emergencies can occur at any point during disease and may be the initial presenting manifestation. These emergencies are not limited to malignancies, as pathologically benign tumors may also present emergently causing life-threatening bowel, biliary, or ureteral obstruction.[4] The imager's role is critical as prompt diagnosis increases the likelihood of a positive outcome.

The imaging manifestations of oncologic emergencies can be categorized into distinct patterns affecting the vascular, biliary, bowel, and genitourinary systems. CT will be emphasized as the modality of choice for most oncologic emergencies; however, there are often ancillary roles for ultrasound for initial screening, as well as nuclear medicine studies and MRI for further characterizing previously detected abnormalities. In addition to imaging findings, common clinical presentations will be discussed, as correlation with signs and symptoms adds value to the radiologist's report and facilitates future imaging.

Vascular

Hemoperitoneum

Spontaneous hemoperitoneum can occur in hypervascular tumors such as hepatocellular carcinoma (HCC), angiosarcoma, pancreatic solid pseudopapillary tumor (SPT), and neuroendocrine tumors. In high HCC-prevalent regions of Asia and Africa, lifetime incidence of spontaneous hemorrhage from HCC can be as high as 14%.[5] Rarely, hematogenous malignancies can present with intraperitoneal hemorrhage secondary to coagulopathy. Patients often present with diffuse abdominal pain due to peritoneal inflammation by blood. Larger volume hemorrhages result in hypovolemia, with nausea, hypotension, tachycardia, and eventually shock. Laboratory values may show drop in hematocrit; however, values are often normal. CT is, therefore, critical in diagnosis.

Imaging will demonstrate variable attenuation of blood products depending on acuity. Anemia or dilution by ascites may also decrease attenuation, with typical density of 35 to 45 HU.[6] While presence of hemoperitoneum can be detected by noncontrast CT, localizing the source of hemorrhage is facilitated by intravenous contrast administration (**Figure 1**). Most abdominopelvic CT imaging in the setting of acute abdominal pain will be performed in the portal venous phase, which can identify the presence of hemoperitoneum, as well as demonstrate the sentinel clot sign, which may help localize the likely site of active bleeding. Clotted blood is of higher attenuation (45 to 70 HU), which will stand out against the background of nonclotted blood. Imaging in the arterial phase with CT angiography (CTA) can demonstrate and localize active arterial extravasation and guide further treatment by surgical or interventional radiology teams.

Trauma may complicate interpretation because certain tumors are more vulnerable to injury than adjacent normal parenchyma. For instance, a small liver HCC could potentially hemorrhage after minor blunt trauma and be misinterpreted as a laceration. A spleen that is enlarged due to lymphoma involvement is similarly at increased risk for rupture.[7] Careful review of history and ancillary findings aids appropriate diagnosis.

Immediate treatment consists of intravenous infusion of fluids and blood products to improve hemodynamic stability. Correction of coagulopathy is also attempted to the extent possible with platelets and clotting factors. Surgery or targeted embolization should

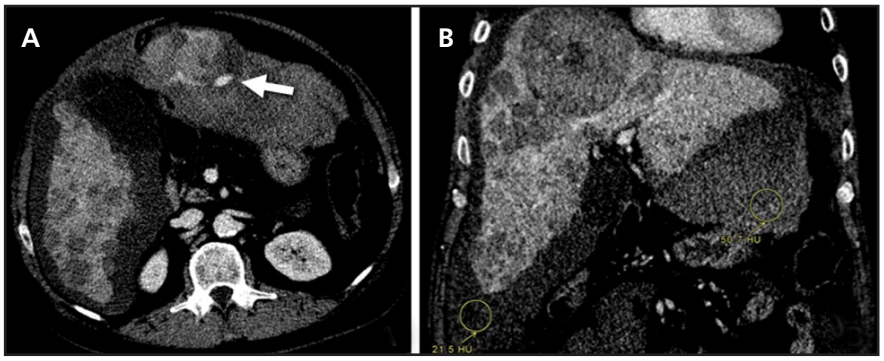

FIGURE 1. *Spontaneous hemoperitoneum in a 60-year-old man with multifocal HCC. Axial CTA image (A) demonstrates active extravasation of contrast from the left lobe after minor trauma (arrow). Coronal CTA image (B) in the same patient shows the sentinel clot sign, which is useful for gross localization of a site of bleeding. Note the higher density of free fluid adjacent to the site of hemorrhage (51 HU) compared to that adjacent to the right lobe of the liver (22 HU). The site of hemorrhage could not be identified on angiography, but the left hepatic artery was empirically embolized based on the CTA findings.*

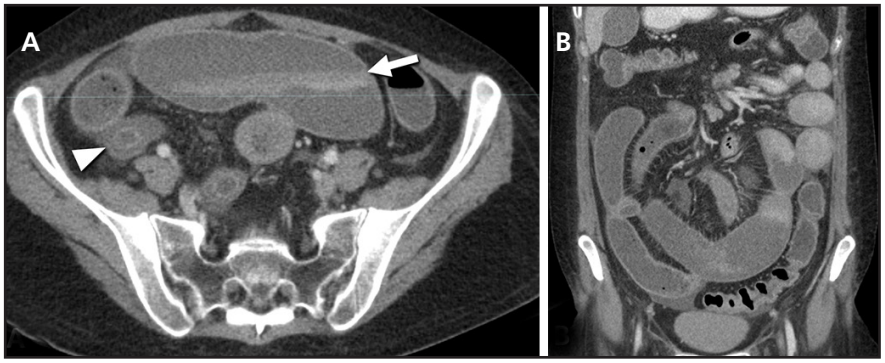

FIGURE 2. *Massive GI bleeding in an 18-year-old patient with AML and steroid-refractory graft-vs-host disease. Noncontrast axial (A) and coronal (B) CT images demonstrate fluid-fluid levels with layering hematocrit (arrow) throughout nearly all loops of the small bowel, which represent blood. No oral contrast was administered. The bowel is diffusely dilated and demonstrates intermittent long-segment mural thickening (arrowhead).*

also be considered for focal masses with life-threatening hemorrhage.

Acute Gastrointestinal Hemorrhage

Malignancy is an uncommon cause of gastrointestinal (GI) bleeding, comprising approximately 7% of lower GI bleeds.[8] Focal hemorrhage due to cancer in the bowel is almost exclusively due to primary adenocarcinoma, which causes diffuse mucosal ulceration and/or erosion into adjacent vessels. Rare hemorrhages caused by direct vascular invasion by other aggressive abdominal tumors (such as HCC or pancreatic adenocarcinoma) have been reported.[9] Hemorrhage over a long segment of bowel may also occur as a consequence of treatment for hematologic disease. Twenty percent of patients with graft vs host disease (GVHD) after allogenic marrow transplant will suffer from diffuse or long segment moderate-severe GI bleeding, usually from the small bowel.[10]

Gastrointestinal hemorrhage secondary to cancer is frequently low volume and not radiographically evident.[11] A hemorrhage rate of at least 0.35 ml/min is typically required for CTA detection, which will demonstrate focal hyperdense contrast extravasation within the bowel lumen.[12] A circumferential or focal mass in the bowel may be detected; however, these are often small. When utilizing CTA to evaluate for acute GI bleed, it is imperative that oral contrast not be administered, as it will obscure a typically small volume of intra-arterial contrast extravasating into the lumen. GVHD disease usually results in hyperdense fluid in the bowel due to diffuse oozing of blood. It is accompanied by long-segment small bowel wall thickening and smooth central enhancement (**Figure 2**).

As an alternative to CTA, Tc-99m red blood cell (RBC) scintigraphy is more sensitive for bleeding, requiring a rate of at least 0.2 ml/min to detect active hemorrhage.[12] The longer imaging time of scintigraphy also improves the detection of intermittent bleeds. Imaging of an active bleed will demonstrate accumulation of a radiotracer in the bowel outside of the intravascular compartment (**Figure 3**). Continued imaging may show a radiotracer in transit along the course of the bowel by peristalsis. Despite the increased sensitivity of scintigraphy, CTA is preferred at most institutions because of more accurate localization and improved detection of soft-tissue findings. Of note, some limitations on nuclear medicine exams may improve with hybrid SPECT/CT imaging.

Catheter-directed angiography requires a rate of at least 1 ml/min for diagnostic localization of an active hemorrhage but has the added advantage of allowing concurrent therapeutic embolization.[12] This modality is most useful for cases of massive bleeding (the requirement of transfusion of at least 4 units of blood over 24 hours or hypotension with systolic blood pressure < 90 mm Hg) or when endoscopic management has failed.[13] Both scintigraphy and CTA are useful for guiding interventional radiology, endoscopic, and surgical procedures.

Acute Venous Thrombosis and Thromboembolic Events

Approximately 3% of all cases of acute mesenteric thrombosis affect the veins, and malignancy is found in a subset of 4% to 16% of these cases (most commonly myeloproliferative disorders).[14,15] Mesenteric thrombosis is much less common than deep venous thrombosis and pulmonary embolism, but shares the common mechanism of over-expression of procoagulant factors by both tumor cells and noncancerous

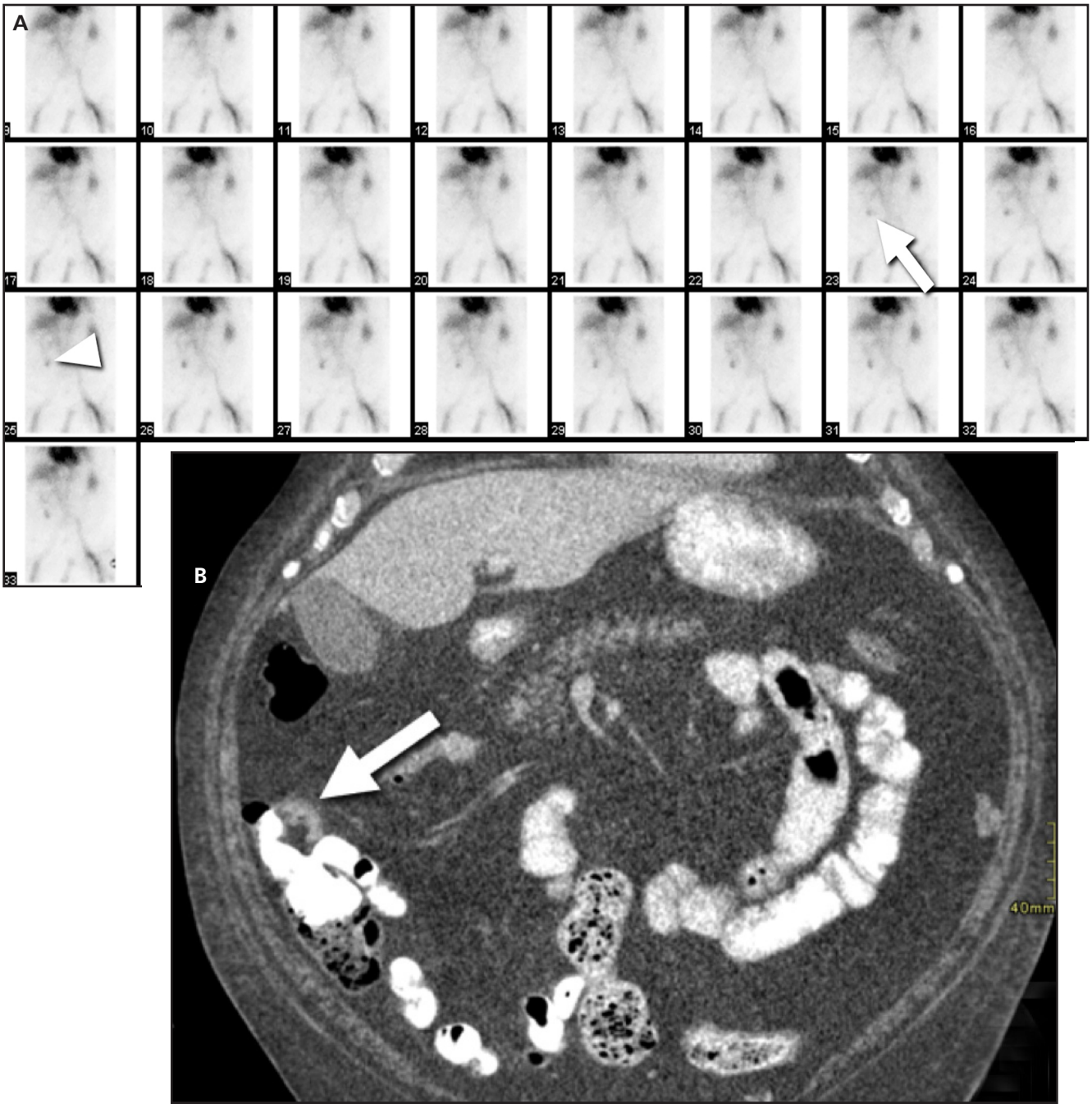

FIGURE 3. *Spontaneous focal GI hemorrhage in a 74-year-old man with colonic adenocarcinoma. Tc-99m (RBC) scintigraphy examination (A) demonstrates appearance of focal activity in the region of the ascending colon (arrow), which slowly accumulates over time and is seen peristalsing toward the hepatic flexure in subsequent images (arrowhead). In the same patient, contrast-enhanced coronal CT (B) with oral contrast demonstrates a small area of thickening and luminal narrowing above the ileocecal valve (arrow), which might not have been detected without localization by scintigraphy. Biopsies from colonoscopy demonstrated primary colonic adenocarcinoma. After stabilization the patient was treated definitively by hemicolectomy.*

tissue. The classic clinical presentation is pain out of proportion to physical examination findings, which begin with subtle distension and blood in the stool.

Findings are occasionally difficult to identify on CT, with retrospective studies indicating at least 90% accuracy in diagnosis of venous mesenteric thrombosis.[14] On portal venous phase contrast-enhanced CT, the filling defect in the mesenteric vasculature appears as a central hypodensity with enhancement of the wall of the affected vessel. Other potential associated findings include portal venous thrombosis and those of intestinal infarction, typified by bowel hypoenhancement, wall thickening, and pneumatosis intestinalis. Although it is rarely considered, catheter-directed mesenteric angiography can be performed in indeterminate cases and

FIGURE 4. *Portal venous and focal aortic thrombosis in a 58-year-old woman with metastatic mucinous adenocarcinoma of the colon on bevacizumab. Axial contrast-enhanced CT of the abdomen demonstrates filling defects in both the left portal vein (arrow) and eccentrically within the lumen of the aorta (arrowhead). The thrombi gradually resolved on subsequent studies with pharmacologic anticoagulation.*

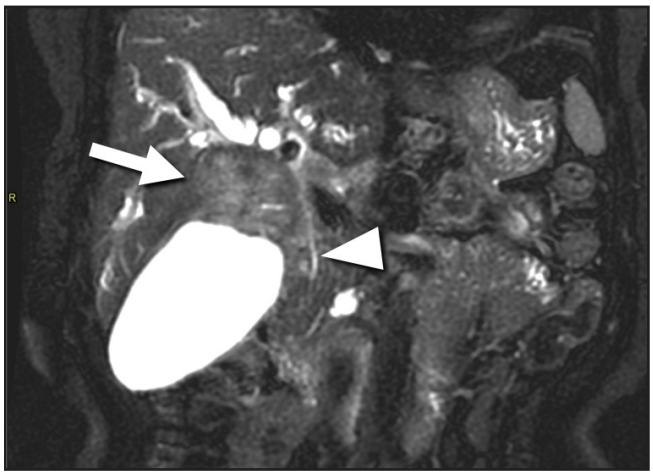

FIGURE 5. *Biliary obstruction in a 69-year-old woman with cholangiocarcinoma. T2-weighted MRI of the abdomen in the coronal plane demonstrates a large mass (arrow) at the neck of the dilated gallbladder obstructing the intrahepatic biliary ducts at the hilum. The distal CBD (arrowhead) is unobstructed.*

would demonstrate a filling defect with late opacification of the proximal vein.[16]

Treatment with anti-angiogenic agents has also been shown to result in arterial and/or venous thrombotic events (**Figure 4**).[17] This is most common in patients treated with bevacizumab for metastatic colorectal cancer, with relative risks of 1.3 for venous and 1.6 for arterial thromboembolic events.[18] The exact mechanism by which thrombosis occurs is not clear, but theories propose that inhibition of VEGF increases vascular inflammation and viscosity/platelet aggregation.

Overall patient survival is better for venous ischemia compared to arterial ischemia but will depend on the specific course of the patient's cancer.[19] Those with limited disease can be treated with systemic anticoagulation and bowel rest, while emergent surgical resection is indicated when bowel infarction has occurred.

Pancreaticobiliary

Obstruction

Pancreatic, ampullary, duodenal, bile duct, and hepatic tumors can result in pancreaticobiliary obstruction, usually by direct invasion or compression of the ducts. Typically, common bile duct (CBD) obstruction is caused by pancreatic ductal adenocarcinoma, followed by invasive cholangiocarcinoma and gallbladder carcinoma. However, any sufficiently large tumor can obstruct ducts by mass effect (**Figure 5**). Fifty-five percent of patients with pancreatic ductal adenocarcinoma will present with jaundice due to conjugated hyperbilirubinemia, which progressively worsens as the obstruction becomes complete.[20] Although the classically suspicious symptom for cancer is painless jaundice, 79% of patients with pancreatic ductal adenocarcinoma present with epigastric pain. Left untreated, obstruction may lead to cholangitis.

The initial imaging test ordered to evaluate obstruction will depend on clinical suspicion. CT is comparable to endoscopic retrograde cholangiopancreatography (ERCP) in establishing the presence of malignant extrahepatic obstruction. In addition to being noninvasive, CT can show ancillary findings such as metastases. Ultrasound is significantly worse for diagnosis (sensitivity of 57%); however, due to its low cost it may be used as the initial study when benign disease is suspected.[21] When no obvious mass is identified, MR cholangiopancreatography (MRCP) should be considered.

Strict size criteria for diagnosing CBD dilation are controversial; however, a simple formula of 6 mm plus 1 mm for each decade after age 60 is generally accepted.[22] The size of the common bile duct may also be increased after cholecystectomy, with potential normal dilation of up to 10 mm.[23] Intrahepatic ductal dilation can be defined as ductal size > 2 mm or > 40% of the adjacent portal vein.[24] Dilation of both the intra- and extrahepatic ducts is more suspicious for obstructing malignancy than dilation of the extrahepatic ducts alone. Dilation of intrahepatic ducts alone may suggest a hilar or intrahepatic malignancy.

Endoscopic stenting may be initially used as a bridge to surgery, or for palliation in patients with unresectable disease. Stents do not interfere with the ability to perform subsequent pancreaticoduodenectomy. Strictures that cannot be traversed with an internal drain require percutaneous external biliary drain placement to decompress the biliary ducts.[25]

Cholecystitis

Gallbladder carcinoma is a rare malignancy that rarely causes acute cholecystitis. Adenocarcinoma represents 90% of cases, with the remainder consisting of squamous, adenosquamous, lymphoma, small cell, and sarcoma malignancies. The rate of incidental gallbladder carcinoma in patients undergoing cholecystectomy for acute cholecystitis in the US is

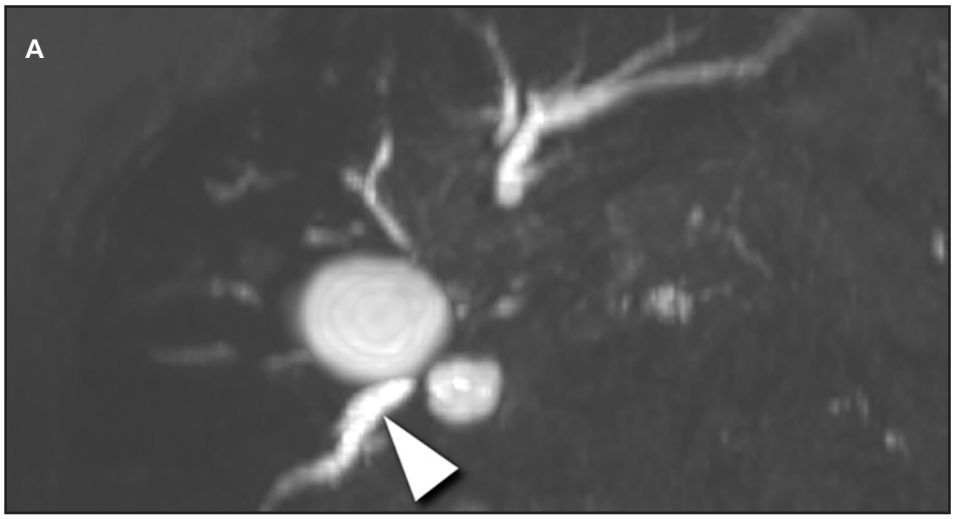

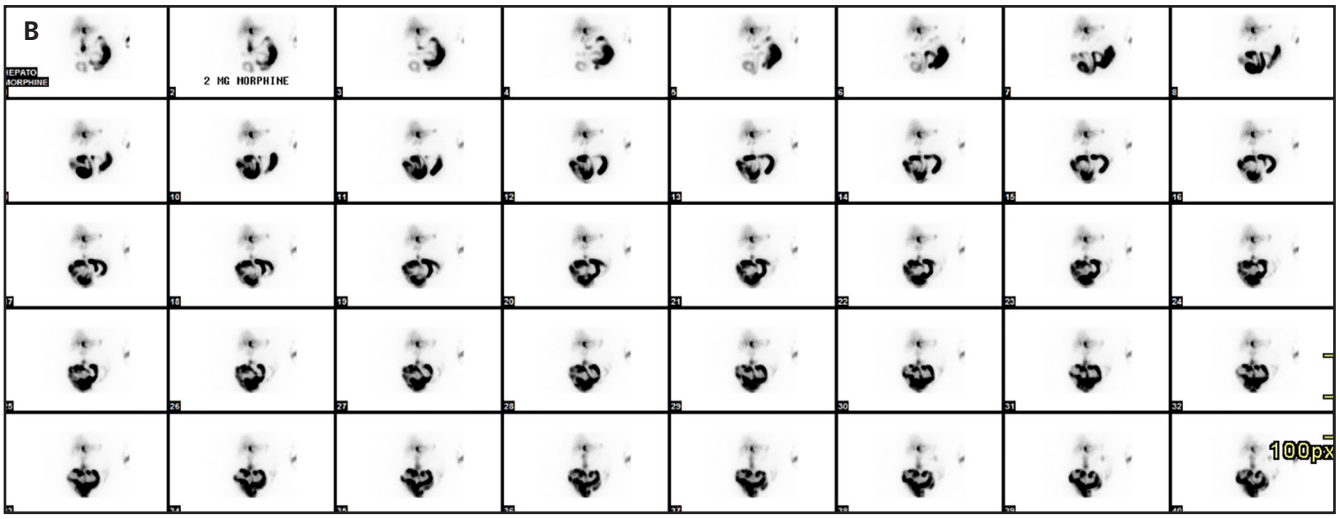

FIGURE 6. *Acute cholecystitis in a 77-year-old woman with gallbladder adenocarcinoma. T2-weighted coronal maximum intensity projection MRI (A) demonstrates nonvisualization of the cystic duct. Prominence of the adjacent intrahepatic ducts (arrowhead) is also evident. HIDA scan (B) in the same patient demonstrates nonvisualization 40 minutes after the administration of intravenous morphine, indicating cystic duct obstruction.*

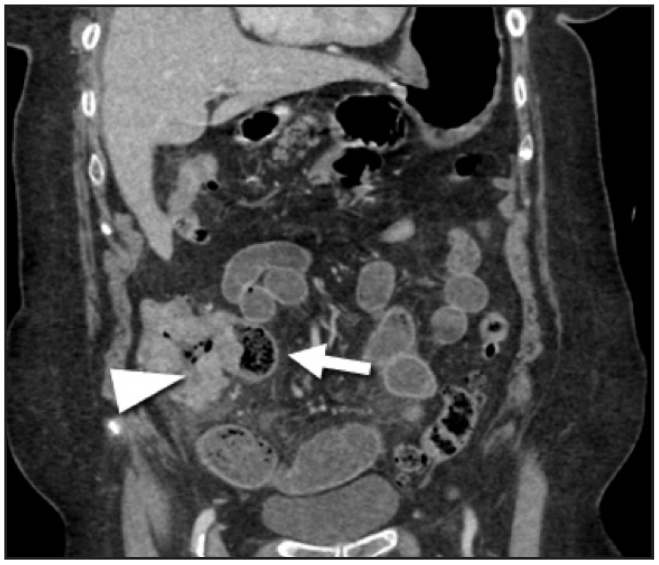

FIGURE 7. *Small bowel obstruction in an 88-year-old woman with adenocarcinoma. Coronal contrast-enhanced CT shows an enhancing cecal mass (arrowhead) at the ileocecal valve with dilation and fecalized contents of the terminal ileum (arrow). Note fat stranding of the adjacent mesentery.*

approximately 0.5% but may be as high as 2.3% in East Asia.[26] As symptoms are related to cystic duct obstruction by the tumor, they closely mimic symptoms of calculous cholecystitis, with acute right upper quadrant pain, fever, and Murphy's sign.

Gallbladder carcinoma is usually advanced at presentation and has a propensity for invading the adjacent liver (**Figure 6**). Many cases present with metastases or bulky porta hepatis and para-aortic lymphadenopathy, with only 25% of these treated with potentially curative resection.[27] A minority of patients with gallbladder carcinoma have subtle findings, which can make prospectively differentiating acute cholecystitis from early gallbladder cancer difficult. A small study has demonstrated that elevated C-reactive protein level and less regional fat stranding are reliable indicators of gallbladder cancer, while cholelithiasis and leukocytosis are not.[28] Irregular wall thickening was useful when present, but only 20% of cancers were polypoid in morphology with the rest infiltrative. The presence of cholelithiasis is not a useful discriminating factor because most patients with gallbladder cancer have gallstones—in fact, larger stones and longer duration of cholelithiasis are both major risk factors for developing gallbladder carcinoma.[29]

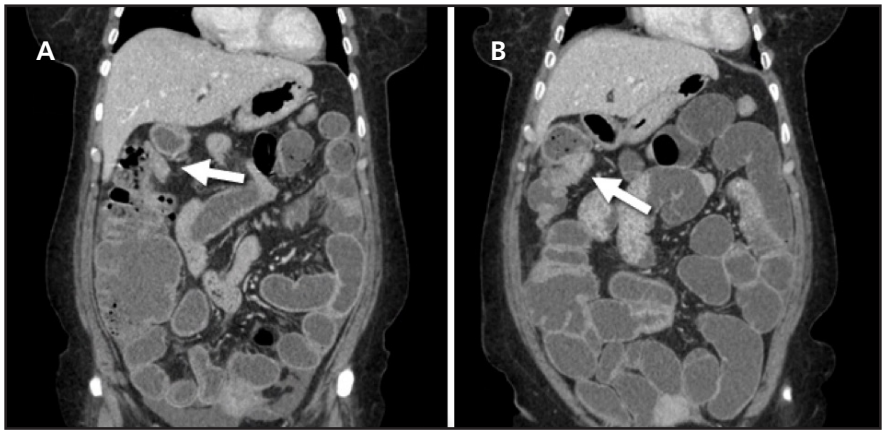

FIGURE 8. *Large and small bowel obstruction in a 56-year-old man with colonic adenocarcinoma. Coronal contrast-enhanced CT (A) shows a large bowel obstruction with secondary dilatation of small bowel, with a transition at the hepatic flexure (arrow). Symptoms were thought to be due to infectious or inflammatory enterocolitis because of the patient's relatively young age, and no follow-up colonoscopy was performed. Repeat CT (B) 6 months later for similar symptoms demonstrates worse distension throughout the proximal bowel, with a more obvious soft-tissue mass at the transition site (arrow). The patient was found to have invasive adenocarcinoma with metastases to the lungs.*

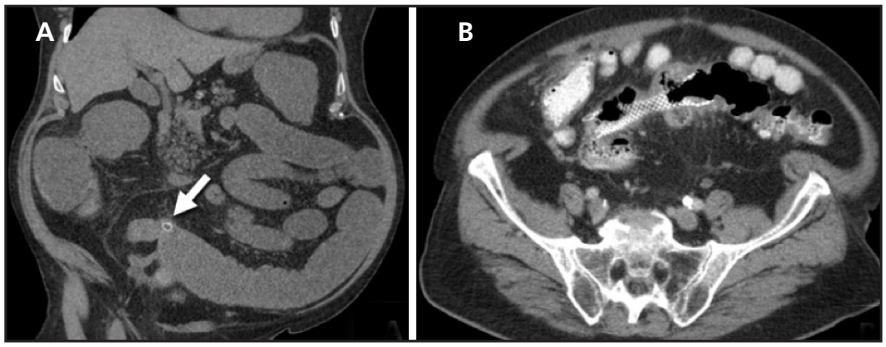

FIGURE 9. *Large bowel obstruction in an 82-year-old patient with sigmoid colon adenocarcinoma. Initial coronal noncontrast CT (A) demonstrates a sigmoid colon stricture of uncertain etiology with small fecalith (arrow). Symptoms did not resolve with conservative treatment and a biopsy from a decompressive sigmoidoscopy demonstrated adenocarcinoma. Subsequent axial CT with oral contrast (B) demonstrates adequate decompression after endoscopic stent placement.*

While white blood cell (WBC) counts tend to be higher in acute cholecystitis by itself, WBC counts are also usually abnormal in gallbladder carcinoma with acute cholecystitis due to acute inflammation.[30]

Cholecystitis in the setting of gallbladder malignancy may be addressed definitively by surgery in certain circumstances. Simple laparoscopic cholecystectomy is considered appropriate for T1a disease, with cure rates ranging from 85% to 100% if negative margins are attained. Only retrospective studies are available as to outcomes for more advanced disease; however, most show that more radical surgery portends better outcomes.[31] An extended cholecystectomy at a minimum involves resection of a rim of hepatic segments IVb and V. T4 disease, which invades the main portal vein, hepatic artery, or multiple extrahepatic organs, is unresectable and best suited to palliative care such as cholecystostomy.

Cholecystitis has also been reported in a small number of cases as a treatment-related side effect from immune checkpoint inhibitor therapy. In contrast to cystic duct obstruction by invasion or compression, the cause is believed to be an autoimmune-related inflammatory state in the gallbladder. These cases were seen in association with drugs targeted to the PD-L1 / PD-1 and CTLA-4 pathways. The role of steroids has not yet been defined, so these cases are managed similarly to cases of typical cholecystitis.[32]

Bowel

Obstruction

Malignancy is a common cause of obstruction of both the small and large bowel. Approximately 20% of small bowel obstructions are due to tumors, predominantly metastases from ovarian, colonic, pancreatic, and gastric neoplasms.[33] Of primary small bowel tumors resulting in obstruction, gastrointestinal stromal tumors (GIST) are most common, followed by lymphoma and adenocarcinoma.[34] In the large bowel, roughly 70% of all obstructions are due to neoplasm, with almost one-fifth of all cases of colon cancer complicated by obstruction at some point. Usually this is due to locally advanced but resectable primary adenocarcinoma. A minority of bowel obstructions occur with lymphoma and noncolonic neoplasms such as pancreatic and ovarian cancer.[35] Patients with acute obstruction will present with abdominal distension, signs of dehydration, and a tympanic abdomen. Often the slow growth of tumors leads to an insidious onset with postprandial discomfort and nausea leading up to acute complete obstruction.

Radiography of acute small bowel obstruction demonstrates dilated bowel loops with air-fluid levels; however, contrast-enhanced CT has become the imaging modality of choice.[36] CT better shows the location, severity, etiology, and complications of obstruction. Classically, the tumor is located in the ileum and results in enhancing short segment thickening of the bowel wall, with upstream dilation. Masses often serve as a lead point for intussusception, which produces a bowel-within-bowel appearance. The small bowel feces sign (**Figure 7**) appears as gas and particulate matter just proximal to the mass, pointing to the site of obstruction.[37]

In the large bowel, the classic obstructing tumor is in the rectosigmoid colon, the same location for the most common nonmalignant source of large bowel obstruction, sigmoid volvulus. Because of the colon's greater capacity to distend, adenocarcinoma classically produces a circumferential "apple core"

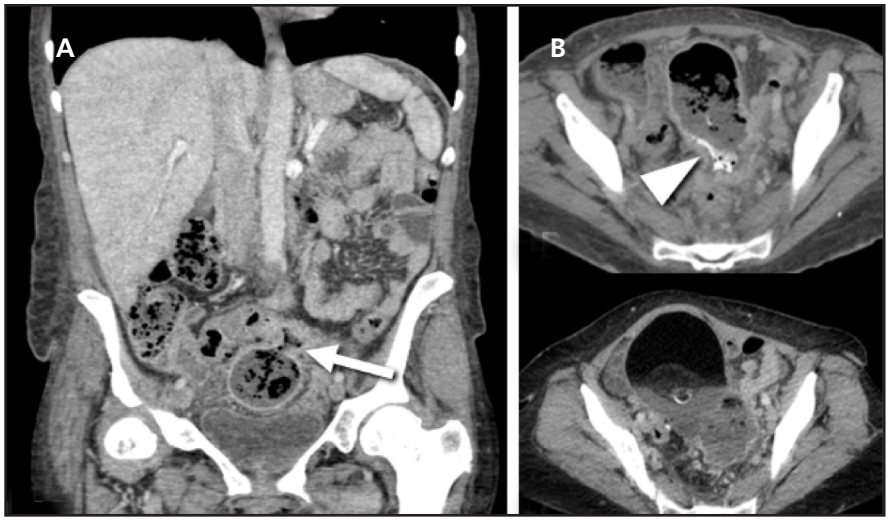

FIGURE 10. *Tumor bowel fistula (TBF) in a 55-year-old woman with a history of mature cystic teratoma. Coronal contrast-enhanced CT (A) demonstrates a heterogenous air-filled mass in the central pelvis superior to the urinary bladder. There is a tract (arrow) connecting to the nearby sigmoid colon, suspicious for TBF. Subsequent axial CT image acquired after the administration of oral contrast (B) shows that contrast (arrowhead) passes from the bowel into the pelvic mass. An axial CT performed 3 months earlier (C) shows that the mature cystic teratoma initially measured > 16 cm. After development of the TBF, most of its contents passed into the large bowel.*

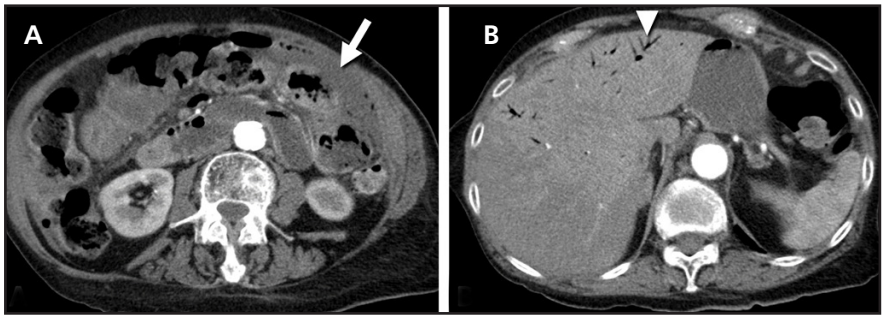

FIGURE 11. *Spontaneous colonic perforation in a 73-year-old woman with history of adenocarcinoma of the lung metastatic to the liver, on chemotherapy. On axial CTA (A), there is free fluid (arrow) and air on the left adjacent to a mural defect in the transverse colon, compatible with perforation. More cranial axial image demonstrates portal venous gas (arrowhead) in the liver, an ominous sign of bowel ischemia. The patient was not considered a surgical candidate and died 18 hours later.*

lesion (**Figure 8**). Upstream dilation varies but can measure > 8 cm proximal to the transition point.[38]

Emergent surgery should be performed in cases where perforation or ischemia is evident, manifested by pneumatosis intestinalis or portal venous gas.[39] In the large bowel, flexible sigmoidoscopy, often with endoscopic stenting (**Figure 9**) appears reasonably successful for preoperative decompression or palliation.[40]

Ischemia, Perforation, and Fistula

These rare GI oncologic complications can occur spontaneously but are increasingly likely to be related to targeted drug and radiation treatments. The complications of ischemia, perforation, and fistula share several common suspected mechanisms related to pressure necrosis, mural infiltration by malignant cells, and/or inflammation due to radiation and chemotherapy.[41] Patients will usually present with abdominal pain, nausea, and fever. Of note, as many as 12.5% of patients with tumor-bowel fistulas will be asymptomatic at diagnosis. Intravenous and oral contrast-enhanced CT is the imaging study of choice.

The most common causes of tumor-bowel fistulas (TBF) are bulky cervical, ovarian, and colon cancers. Primary small bowel tumors and lymphoma are rarely associated. Tumor size is the primary risk factor, with case studies reporting 8 to 26 cm.[42] Another important risk factor is chemoradiotherapy. A case study of 2096 cervical cancers found that all 38 patients who developed TBFs had undergone prior radiation therapy.[43] TBF should be suspected on imaging when gas is present within a tumor; however, gas may also be a sign of bacterial infection. In unclear cases, the administration of oral contrast allows for a more confident diagnosis when contrast is seen extending into the tumor. A tract between the tumor and nearby bowel can often be appreciated on reformats (**Figure 10**).

The risk of tumor-related perforation is highest in ovarian, pancreatic, colon, and rectal cancers. Molecular targeted therapy with antiangiogenic drugs is particularly associated with perforation, and to a lesser extent, fistula. For instance, treatment with bevacizumab (a monoclonal antibody which inhibits VEGF-A) carries a risk of bowel perforation between 1% and 4%.[44] On imaging, gas and fluid are usually proximal to the site of perforation (**Figure 11**). Large bowel perforations can result in massive pneumoperitoneum, whereas small bowel perforations can be more difficult to detect. In some cases, the gas remains closely localized to the site of perforation due to containment by inflammatory reaction.

Early discontinuation of treatment is important for initial treatment of both TBF and perforation, as stopping molecular targeted therapy is associated with reversal of pneumatosis.[45] Definitive management requires surgical resection, but conservative management can be attempted in the absence of peritonitis or sepsis.

Genitourinary

Urinary Tract Obstruction

In addition to urothelial cell carcinoma (UCC), urinary tract obstruction occurs often in patients with a variety of malignancies involving the retroperitoneum and pelvis including colon, ovary,

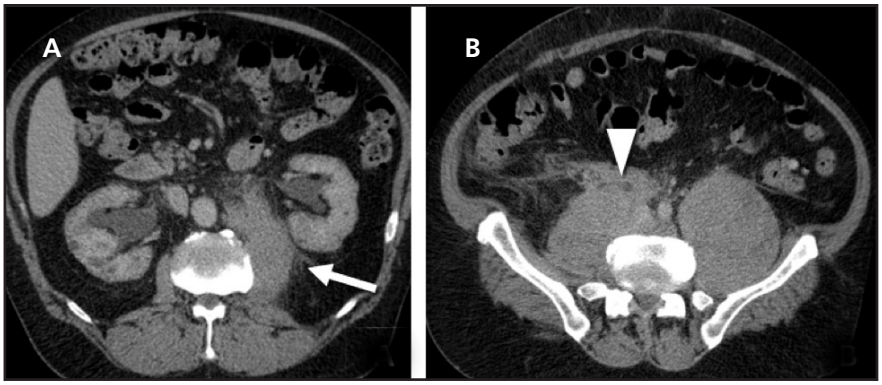

***FIGURE 12**. Bilateral ureteral obstruction in a 58-year-old patient presenting with spontaneous tumor lysis syndrome from previously undiagnosed "double hit" B-cell lymphoma. Axial noncontrast CT (A) demonstrates bilateral hydronephrosis. The left psoas is enlarged and indistinct (arrow), indicating its involvement by lymphoma. There are several enlarged retroperitoneal lymph nodes. An axial CT image (B) of the abdomen more inferiorly demonstrates encasement of the dilated right ureter (arrowhead) by lymphoma.*

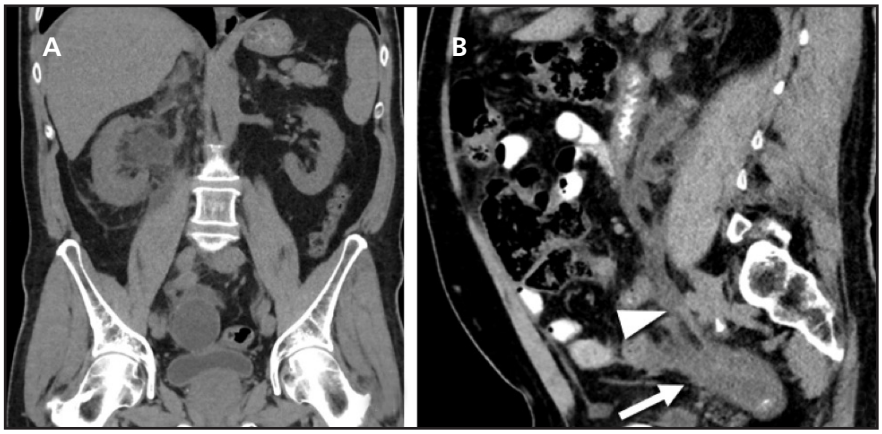

***FIGURE 13.** Unilateral ureteral obstruction in a 66-year-old man with poorly differentiated adenocarcinoma thought to be arising from an appendiceal mucocele. There is unilateral right hydroureteronephrosis seen on coronal noncontrast CT (A). Sagittal CT with oral and intravenous contrast (B) shows ureteral dilation that terminates at the site of irregular mural thickening (arrowhead). The stricture is surrounded by fat stranding and is in proximity to the heterogenous mass arising from the appendix (arrow).*

and prostate neoplasms causing direct invasion or compression. Malignant urinary obstruction is an ominous development, with a median survival time of 3 months.[46] Lymphoma/lymphadenopathy less commonly results in obstruction (**Figure 12**). Primary urothelial cell carcinoma (UCC) of the ureter is exceedingly rare, occurring approximately 100 times less frequently than UCC of the bladder. In addition to pain, patients are at high risk for developing sepsis related to obstruction and may also develop hypertension from electrolyte and water retention. Symptoms are variable depending on the acuity of obstruction. When due to unilateral external compression, patients are often initially asymptomatic because of the slow progression of disease.

In order of increasing preference, ultrasound, CT without contrast, contrast-enhanced CT, and CT/MR urography can be used to image malignant obstruction. Noncontrast CT and ultrasound are often performed in the emergent setting because of concurrent acute renal failure, prohibiting the use of intravenous contrast. While any portion of the collecting system can be involved, the distal third of the ureter is a frequent site (**Figure 13**).[47] Proximally, the collecting system will be dilated with the kidney demonstrating a delayed nephrogram on contrast-enhanced CT. A delayed nephrogram (**Figure 14**) appears as reduction of the normal renal parenchymal enhancement in the later phases of contrast excretion (the time point when venous-phase CT is performed). An infiltrating mass with adjacent fat stranding will often be seen in the renal pelvis or ureter in cases of UCC, occasionally appearing as an intrarenal mass when arising in a more proximal calyx. If no definite mass is identified, then irregular narrowing of the ureteral lumen can be a helpful sign.[48] Although infrequently performed by radiologists, retrograde pyelography may show contrast within the interstices of a UCC (stipple sign) and distal cupping of intraluminal tumor by contrast (goblet sign).

The three general categories of treatment for acute genitourinary obstruction are: palliation, treatment of extrinsic compression, and surgery. In the case of obstruction by metastasis, the usual approach is by palliation of symptoms with retrograde placement of a ureteric stent. If this cannot be accomplished, percutaneous nephrostomy catheter placement will relieve the obstruction but is more invasive and requires an external drainage bag. For extrinsic compression, treatment of the offending mass should resolve the obstruction; however, stents or nephrostomy tubes may be used as temporizing measures. Lastly, ureteral diversion surgeries can be considerered.[47]

Acute Adnexal Torsion

Ovarian cysts and masses are the primary risk factors for adnexal torsion. Two case series of patients with ovarian torsion found that 31% to 46% had an ovarian mass, with most of the remainder having simple and hemorrhagic cysts.[49,50] Torsion is overwhelmingly more likely to occur in patients with benign masses. A potential explanation is that malignant masses preferentially develop a fixating desmoplastic reaction. Acute adnexal torsion is most likely to occur in patients of reproductive age. Pregnant patients are at particular risk, probably due to hypermobile ligaments.[51] Patients present with acute

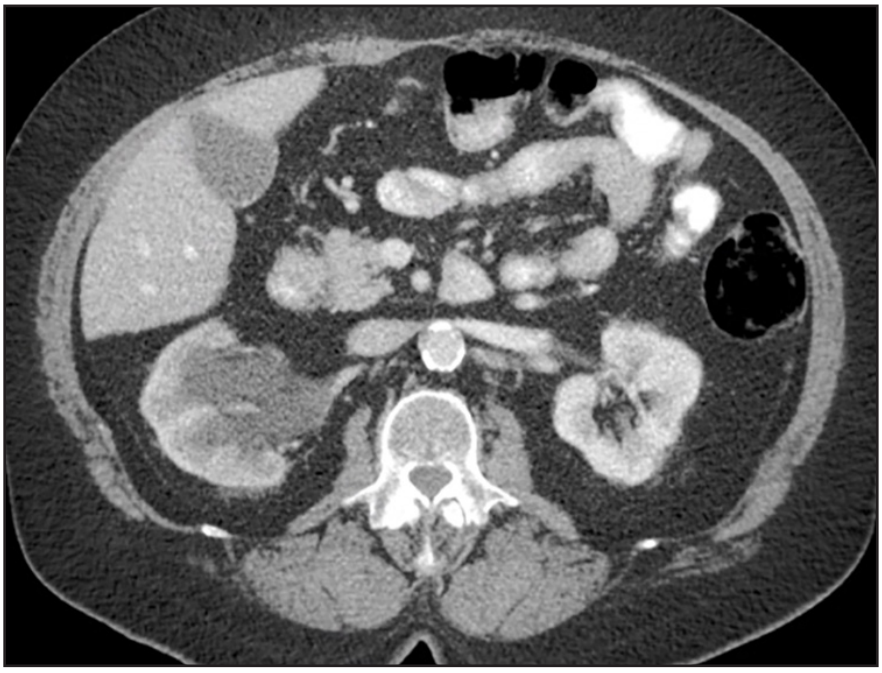

FIGURE 14. *Delayed nephrogram in a 63-year-old woman with colon cancer and peritoneal metastases. Contrast-enhanced CT demonstrates decreased attenuation of the right kidney due to obstruction by metastasis (not pictured) and poor contrast uptake. Scattered peritoneal metastases measuring < 5 mm are present.*

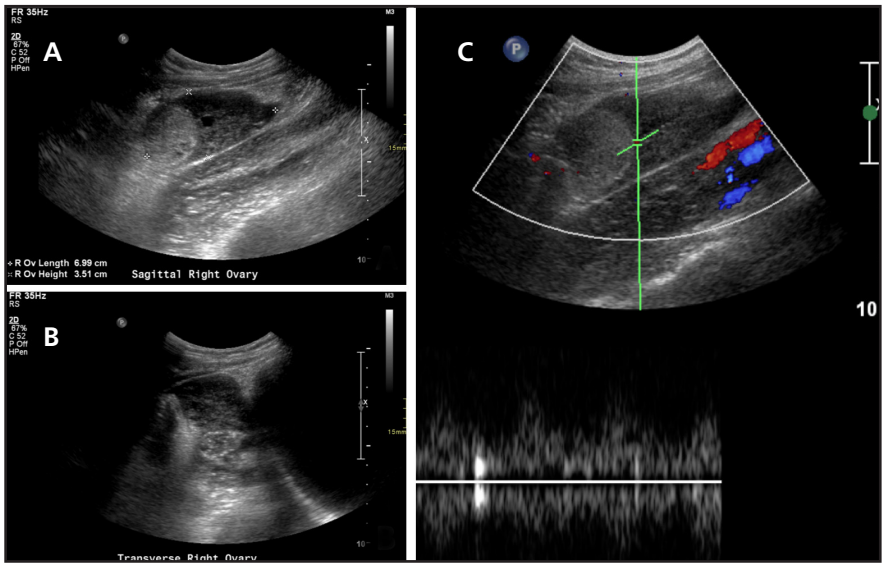

FIGURE 15. *Acute adnexal torsion in a 15-year-old girl with an ovarian mature cystic teratoma. Grayscale ultrasound demonstrates a heterogenous, enlarged right ovary that contains an echogenic, poorly defined mass on sagittal (A) and transverse (B) grayscale images. The patient was found to have acute torsion on surgery, with a 15-cm mature cystic teratoma serving as the lead point. Spectral Doppler ultrasound (C) demonstrates the presence of arterial waveforms in the morphologically abnormal ovary.*

pelvic pain, nausea, and sometimes fever. The pain may be intermittent due to spontaneous detorsion and retorsion.

Initial investigation for torsion should be performed by ultrasound. The most reliable finding on ultrasound is an enlarged ovary, measuring > 20 ml in volume or > 4 cm in greatest dimension. The ovary may also demonstrate stromal edema and heterogeneity due to vascular outflow obstruction. An infrequent but specific sign for adnexal torsion is the twisted vascular pedicle (whirlpool sign). This manifests as a hyperechoic mass adjacent to the ovary with central hypoechoic vessels, sometimes with a beak-like interface. Unlike in the testes, arterial spectral Doppler waveforms may be preserved because of its dual-ovarian blood supply from uterine collaterals and the ovarian artery. Masses serving as lead points will have variable imaging appearance. Mature cystic teratoma is the most common mass seen in torsion, with benign serous cystadenoma slightly less likely (**Figure 15**).[52]

While CT should not be performed as the primary modality in cases of suspected ovarian torsion, it may be the first line of imaging when symptoms and history are atypical. In addition to the ovary appearing enlarged and displaced, the uterus is often displaced toward the side of torsion. In less than one-third of cases, a twisting of the vascular pedicle in the affected adnexa can be visualized. Absent enhancement is a worrying sign for infarction of the ovary. MRI is not typically utilized in the emergent setting due to the ease of ultrasound but demonstrates a similar pattern of findings as described with CT, with T1 hypointense/T2 hyperintense edema.

Adnexal torsion, if not treated promptly, can lead to ovarian necrosis and infertility. Patients with an ovarian mass suspicious for malignancy require salpingo-oophorectomy, whereas benign cysts may be treated with cystectomy and detorsion/fixation of the ovary.[53]

Conclusion

Oncologic emergencies of the abdomen and pelvis are life-threatening events of increasingly common incidence affecting the vascular, pancreaticobiliary, GI, and genitourinary systems. The radiologist should be able to quickly and accurately detect these findings. In patients with known cancer on treatment, clinical information should be integrated into interpretation to identify potential treatment-related emergencies.

References

1. Siegel RL, Miller KD, and Jemal A.Cancer statistics, 2019. CA A Cancer J Clin 2019;69(1):7-34.
2. Morani AC, Hanafy AK, Marcal LP, et al. Imaging of acute abdomen in cancer patients. Abdom Radiol (NY) 2019 Nov 22.
3. Torres VB, Vassalo J, Silva UV, et al. Outcomes in critically ill patients with cancer-related complications. PLoS One 2016;11(10):e0164537.
4. Lewis MA, Hendrickson AW, Moynihan TJ. Oncologic emergencies: pathophysiology, presentation, diagnosis, and treatment. CA Cancer J Clin 2011;61(5):287-314.
5. Casillas VJ, Amendola MA, Gascue A, et al. Imaging of nontraumatic hemorrhagic hepatic lesions. Radiographics 2000;20(2):367-378.
6. Lubner M, Menias C, Rucker C, et al. Blood in the belly: CT findings of hemoperitoneum. Radiographics 2007;27(1):109-125.
7. Bauer TW, Haskins GE, Armitage JO. Splenic rupture in patients with hematologic malignancies. Cancer 1981;48(12):2729-2733.
8. Hreinsson JP, Gumundsson S, Kalaitzakis E, Bjornsson ES. Lower gastrointestinal bleeding: incidence, etiology, and outcomes in a population-based setting. Eur J Gastroenterol Hepatol 2013;25(1):37-43.
9. Hot S, YeşiltaşM, Gökçek B, Egin S, Sengiz S. Massive and life-threatening upper gastrointestinal bleeding due to invasive hepatocellular carcinoma: a case report. Int J Surg Case Rep 2016;26:69-72.
10. Nevo S, Enger C, Swan V, et al. Acute bleeding after allogeneic bone marrow transplantation: association with graft versus host disease and effect on survival. Transplantation 1999;67(5):681-689.
11. Macrae FA, St John DJ. Relationship between patterns of bleeding and Hemoccult sensitivity in patients with colorectal cancers or adenomas. Gastroenterology 1982;82(5 Pt 1):891-898.
12. Geffroy Y, Rodallec MH, Boulay-Coletta I, et al. Multidetector CT angiography in acute gastrointestinal bleeding: why, when, and how. RadioGraphics. 2011;31(3):E35-E46.
13. Ramaswamy RS, Choi HW, Mouser HC, et al. Role of interventional radiology in the management of acute gastrointestinal bleeding. World J Radiol 2014;6(4):82-92.
14. Hmoud B, Singal AK, Kamath PS. Mesenteric venous thrombosis. J Clin Exp Hepatol 2014;4(3):257-263.
15. Schoots IG, Koffeman GI, Legemate DA, et al. Systematic review of survival after acute mesenteric ischaemia according to disease aetiology. Br J Surg 2004 Jan;91(1):17-27.
16. Clark RA, Gallant TE. Acute mesenteric ischemia: angiographic spectrum. Am J Roentgenol 1984;142(3):555-562.
17. Suenaga M, Mizunuma N, Kobayashi K, et al. Management of venous thromboembolism in colorectal cancer patients treated with bevacizumab. Med Oncol 2010;27:807-814.
18. Alahmari AK, Almalki ZS, Alahmari AK, et al. Thromboembolic events associated with bevacizumab plus chemotherapy for patients with colorectal cancer: a meta-analysis of randomized controlled trials. Am Health Drug Benefits 2016;9(4):221-232.
19. Orr DW, Harrison PM, Devlin J, et al. Chronic mesenteric venous thrombosis: evaluation and determinants of survival during long-term follow-up. Clin Gastroenterol Hepatol 2007;5(1):80-86.
20. Porta M, Fabregat X, Malats N et al. Exocrine pancreatic cancer: symptoms at presentation and their relation to tumour site and stage. Clin Transl Oncol 2005;7:189-197.
21. Pasanen PA, Partanen KP, Pikkarainen PH, et al. A comparison of ultrasound, computed tomography and endoscopic retrograde cholangiopancreatography in the differential diagnosis of benign and malignant jaundice and cholestasis. Eur J Surg 1993;159(1):23-29.
22. Bachar GN, Cohen M, Belenky A, et al. Effect of aging on the adult extrahepatic bile duct: a sonographic study. J Ultrasound Med 2003;22(9):879-82; quiz 883-885.
23. Maple JT, Ben-Menachem T, Anderson MA, et al. The role of endoscopy in the evaluation of suspected choledocholithiasis. Gastrointest Endosc 2010;71(1)1-9.
24. Yarmenitis SD. Ultrasound of the gallbladder and the biliary tree. Eur Radiol 2002;12(2):270-282.
25. Coates JM, Beal SH, Russo JE, et al. Negligible effect of selective preoperative biliary drainage on perioperative resuscitation, morbidity, and mortality in patients undergoing pancreaticoduodenectomy. Arch Surg 2009;144(9):841-847.
26. Lam CM, Yuen AW, Wai AC, et al. Gallbladder cancer presenting with acute cholecystitis: a population-based study. Surg Endosc 2005;19:697-701.
27. Fong Y, Jarnagin W, Blumgart LH. Gallbladder cancer: comparison of patients presenting initially for definitive operation with those presenting after prior noncurative intervention. Ann Surg 2000;232(4):557-569.
28. Kim SH, Jung D, Ahn JH, et al. Differentiation between gallbladder cancer with acute cholecystitis: considerations for surgeons during emergency cholecystectomy, a cohort study. Int J Surg 2017;45:1-7.
29. Sharma A, Sharma KL, Gupta A, et al. Gallbladder cancer epidemiology, pathogenesis and molecular genetics: recent update. World J Gastroenterol 2017;23(22):3978-3998.
30 .Jayaraman S, Jarnagin WR. Management of gallbladder cancer. Gastroenterol Clin North Am 2010;39(2):331-342.
31. Bartlett DL, Fong Y, Fortner JG, et al. Long-term results after resection for gallbladder cancer. Implications for staging and management. Ann Surg 1996;224(5):639-646.
32. Abu-Sbeih H, Tran CN, Ge PS, et al. Case series of cancer patients who developed cholecystitis related to immune checkpoint inhibitor treatment. J Immunother Cancer 2019;7:118.
33. Mullan CP, Siewert B, Eisenberg RL. Small bowel obstruction. Am J Roentgenol 2012;198(2):W105-17. doi: 10.2214/AJR.10.4998.
34.Kendrick ML. Partial small bowel obstruction: clinical issues and recent technical advances. Abdom Imaging 2009;34(3):329-334.
35.Kahi CJ, Rex DK. Bowel obstruction and pseudo -obstruction. Gastroenterol Clin North Am 2003;32(4):1229-1247.
36. Katz DS, Baker ME, Rosen MP, et al. ACR Appropriateness Criteria Suspected Small-Bowel Obstruction. https://acsearch.acr.org/docs/69476/Narrative/. American College of Radiology. Accessed November 15, 2019.
37. Tuca A, Guell E, Martinez-Losada E, Codorniu N. Malignant bowel obstruction in advanced cancer patients: epidemiology, management, and factors influencing spontaneous resolution. Cancer Manag Res 2012;4:159-169.
38. Taourel P, Kessler N, Lesnik A, et al. Helical CT of large bowel obstruction. Abdom Imaging 2003;28(2):267-275.
39. Paul Olson TJ, Pinkerton C, Brasel KJ, et al. Palliative surgery for malignant bowel obstruction from carcinomatosis: a systematic review. J Am Med Assoc Surg 2014;149(4):383-92. doi: 10.1001/jamasurg.2013.4059.
40. Cheung HY, Chung CC, Tsang WW, et al. Endolaparoscopic approach vs conventional open surgery in the treatment of obstructing left-sided colon cancer: a randomized controlled trial. Arch Surg 2009;144(12):1127-1132.
41. Tirumani SH, Baez JC, Jagannathan JP, et al. Tumor-bowel fistula: what radiologists should know. Abdom Imaging 2013;38(5):1014-1023.
42. Yahagi N, Kobayashi Y, Ohara T, et al. Ovarian carcinoma complicated by sigmoid colon fistula formation: a case report and review of the literature. J Obstet Gynaecol Res 2011;37(3):250-253.
43. Emmert C, Köhler U. Management of genital fistulas in patients with cervical cancer. Arch Gynecol Obstet 1996;259(1):19-24.
44. Abu-Hejleh T, Mezhir JJ, Goodheart MJ, et al. Incidence and management of gastrointestinal perforation from bevacizumab in advanced cancers. Curr Oncol Rep 2012;14(4):277-284.
45. Saif MW, Elfiky A, Salem RR. Gastrointestinal perforation due to bevacizumab in colorectal cancer. Ann Surg Oncol 2007;14(6):1860-1869.
46. Russo P. Urologic emergencies in the cancer patient. Semin Oncol 2000;27(3):284-298.
47. Allen DJ, Longhorn SE, Philp T, et al. Percutaneous urinary drainage and ureteric stenting in malignant disease. Clin Oncol (R Coll Radiol) 2010;22(9):733-739.
48. Browne RF, Meehan CP, Colville J, et al. Transitional cell carcinoma of the upper urinary tract: spectrum of imaging findings. Radiographics 2005;25(6):1609-1627.
49. White M, Stella J. Ovarian torsion: 10-year perspective. Emerg Med Australas 2005;17(3):231-237.
50. Varras M, Tsikini A, Polyzos D, et al. Uterine adnexal torsion: pathologic and gray-scale ultrasonographic findings. Clin Exp Obstet Gynecol 2004;31(1):34-38.
51 .Tsafrir Z, Hasson J, Levin I, et al. Adnexal torsion: cystectomy and ovarian fixation are equally important in preventing recurrence. Eur J Obstet Gynecol Reprod Biol 2012;162(2):203-055.
52. Lourenco AP, Swenson D, Tubbs RJ et al. Ovarian and tubal torsion: imaging findings on US, CT, and MRI. Emerg Radiol 2014;21:179-187.
53. Anders JF, Powell EC. Urgency of evaluation and outcome of acute ovarian torsion in pediatric patients. Arch Pediatr Adolesc Med 2005;159(6):532-535.

New Saccular Abdominal Aortic Aneurysm

Alex Pavidapha, M.D., Hemang Kotecha, D.O.

Department of Radiology, UMass Memorial Medical Center, Worcester, MA

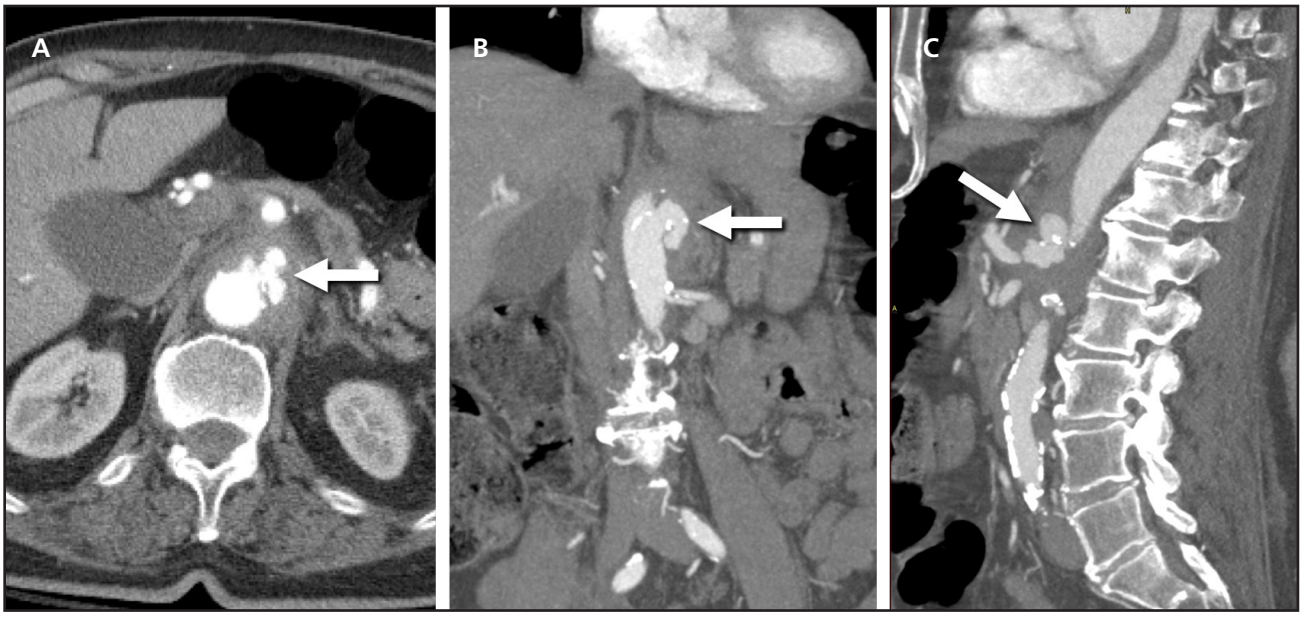

FIGURE 1. *Axial CTA image (A) and coronal (B) and sagittal (C) maximum-intensity projection images show a lobular contrast collection protruding from the suprarenal abdominal aortic lumen (arrows) with periaortic soft-tissue thickening and fat stranding.*

Case Presentation

An 88-year-old man who had been hospitalized 3 months prior for *Staphylococcus aureus* bacteremia and presumed urosepsis presented to the emergency department with acute abdominal pain and acute worsening of chronic back pain. The patient underwent CT of the abdomen and pelvis, followed by a CT angiogram (CTA) (**Figure 1**). A CT performed during a prior hospitalization showed a normal caliber abdominal aorta (**Figure 2**). MRI of the lumbar spine during the hospitalization did not show any evidence of discitis or osteomyelitis (**Figure 3**).

Key Clinical Finding(s)

Worsening back pain
Sepsis

Key Imaging Finding(s)

New saccular abdominal aneurysm with periaortic fat stranding

Differential Diagnosis

Infectious aneurysm (mycotic aneurysm)
Penetrating atherosclerotic ulcer
Inflammatory aneurysm

Discussion

Abdominal aortic aneurysms are defined by a > 50% focal dilation of the abdominal aorta or when the abdominal aortic diameter is > 3 cm.[1-3] Aneurysms can be further classified into the more common fusiform subcategory (accounting for 80% of cases), or the rarer saccular type.[3] Saccular aneurysms are focal and have a more lobular configuration with a narrower neck. If a saccular aneurysm is identified on imaging, the primary differential diagnoses include infected aneurysm, inflammatory aneurysm, and penetrating atherosclerotic ulcer, with or without contained rupture. The role of imaging is for diagnosis and treatment planning. Differentiating a saccular aneurysm from its fusiform counterpart is imperative since

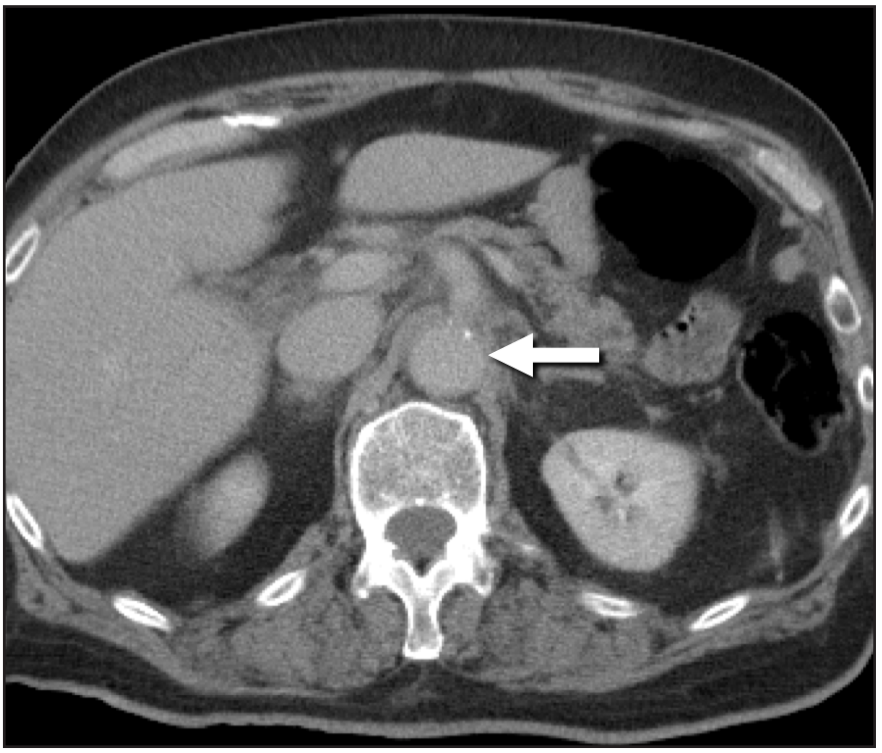

FIGURE 2. *Axial image from contrast-enhanced CT performed 3 months prior shows a normal caliber abdominal aorta (arrow).*

repair is recommended for all saccular aneurysms regardless of size or symptomology.[1] Additionally, certain imaging features such as rapid growth, periaortic soft-tissue stranding, and periaortic fluid can suggest impending rupture.

Differential Diagnosis

Infected Aneurysm (Mycotic Aneurysm)

Infected aneurysms most commonly involve the aorta, with the most common causative organisms being *Staphylococcus*, *Salmonella,* and *Streptococcus* species.[4] An infected aneurysm is defined as infectious disruption in the wall of an artery with development of a saccular protrusion that is contiguous with the lumen of the artery. Development may be secondary to infection of a pre-existing intimal defect, hematogenous spread via the vasa vasorum in a normal or aneurysmal artery, direct spread from trauma or intervention, or contiguous spread from adjacent abscess. Clinical presentation can be widely variable, ranging from life-threatening hemorrhage to being clinically occult. Most patients usually present febrile or septic and with abdominal and back pain.[3]

CTA is the imaging modality of choice for evaluating a suspected infected aneurysm, which manifests as a saccular aneurysm with lobular contours and periaortic soft-tissue enhancement, edema, and stranding. Periaortic gas and adjacent abscess may also be present. The appearance of an infected aneurysm on MRI is similar to that on CT, with periaortic high-signal intensity on T2-weighted imaging (T2WI) and periaortic enhancement after administration of gadolinium-based contrast. Osseous involvement may be better delineated with MRI. Ultrasound is not reliable for diagnosis of infected aneurysms of the abdominal aorta but is utilized for evaluation of peripheral arteries.

FIGURE 3. *Parasagittal short-tau inversion recovery (STIR) image from lumbar spine MRI performed 3 months prior shows a normal caliber abdominal aorta with faint periaortic signal hyperintensity (arrow). No findings indicated vertebral osteomyelitis or discitis.*

Inflammatory Aneurysm

Inflammatory abdominal aortic aneurysms are a variant of typical atherosclerotic aneurysm and are usually fusiform. They are characterized by extensive thickening of the aneurysm wall, perianeurysmal fibrosis or soft-tissue thickening, and adherence to adjacent retroperitoneal structures.[5] Inflammatory aortic aneurysms occur in a younger population of patients than atherosclerotic aneurysms. Patients often present with abdominal or back pain (80% of patients), weight loss, and an elevated erythrocyte sedimentation rate.[2]

On CT, an inflammatory aneurysm typically presents as a fusiform aneurysm with soft tissue surrounding the

aorta. The perianeursymal soft tissue enhances with administration of intravenous contrast, and the degree of enhancement correlates with stage of disease and treatment response. Early and active disease will demonstrate avid enhancement and later stage and chronic disease will have minimal enhancement. In later stages of the disease, there is often inflammatory fibrotic retraction of adjacent structures, including the ureters, which can cause hydronephrosis. On MRI, T2WI will exhibit characteristic high-signal intensity in early/active disease and low-signal intensity in late/chronic disease. In a similar fashion, postcontrast T1-weighted imaging (T1WI) will demonstrate increased enhancement in early/active disease and relatively low enhancement in late/chronic disease.

Penetrating Atherosclerotic Ulcer

Penetrating atherosclerotic ulcers (PAUs) occur from an ulcerated atherosclerotic plaque that penetrates the internal elastic lamina.[6] They are often associated with varying degrees of intramural hemorrhage and can progress to intramural hematoma, dissection, and aortic rupture. PAUs most often develop in the thoracic aorta in patients with advanced atherosclerotic disease.[3]

On CTA, PAUs appear as focal outpouching of contrast beyond the expected margin of the aortic wall in the region of an atherosclerotic plaque. The plaque will often be inwardly displaced and subintimal hematoma may be present.[6] On MRI, mural indentation is surrounded by signal hyperintensity on T1WI and T2WI, owing to the presence of blood products.

Diagnosis

Infected (mycotic) aneurysm

Summary

Identifying and differentiating a saccular aneurysm is of great importance due to the high morbidity and mortality associated with the differential diagnoses when not treated appropriately. Imaging, particularly CTA, is essential for diagnosis and treatment planning for patients with a new or enlarging saccular aneurysm. Imaging findings in conjunction with clinical presentation and laboratory values are important for the differential diagnoses: infected aneurysm, penetrating atherosclerotic ulcer, and inflammatory aneurysm. Thus, an understanding of the patient presentation, disease process, and imaging features is vital for the radiologist.

References

1. Shang, Eric K, Boonn WW, et al. A modern experience with saccular aortic aneurysms. J Vasc Surg 201;57(1):84-88.
2. Tang T, Boyle JR, Dixon AK, Varty K. Inflammatory abdominal aortic aneurysms. Eur J Vasc Endovasc Surg 2005;29(4):353-362.
3. Wadgaonkar AD, Black III JH, Weihe EK, et al. Abdominal aortic aneurysms revisited: MDCT with multiplanar reconstructions for identifying indicators of instability in the pre- and postoperative patient. Radiographics 2015;35(1):254-268.
4. Lee WK, Mossop PJ, Little AF, et al. Infected (mycotic) aneurysms: spectrum of imaging appearances and management. Radiographics 2008;28(7):1853-1868.
5. Hellmann DB, Grand DJ, Freischlag JA. Inflammatory abdominal aortic aneurysm. J Am Med Assoc 2007;297(4):395-400.
6. Hayashi H, Matsuoka Y, Sakamoto I, et al. Penetrating atherosclerotic ulcer of the aorta: imaging features and disease concept. Radiographics 2000;20(4):995-1005.

Pulmonary Nodules Following Renal Transplant

Uday Malhotra, M.D., Gabriela Santos-Nunez, M.D.

Department of Radiology, UMass Memorial Medical Center, Worcester, MA

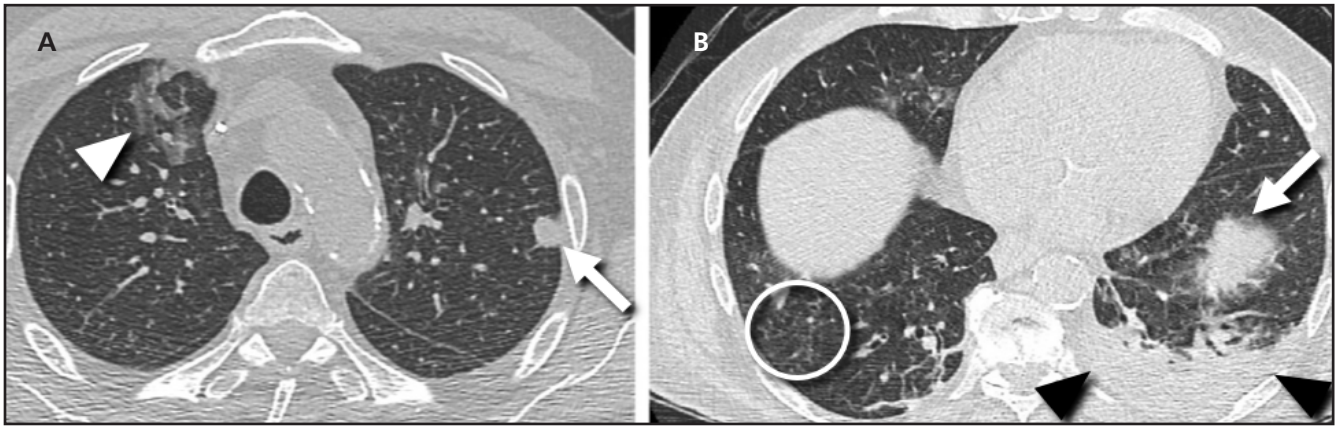

FIGURE 1. *Axial chest CT image (A) demonstrates nodular consolidation in the left upper lobe (arrow) and ground-glass opacities in the right upper lobe (arrowhead). More caudal axial CT image (B) reveals nodular consolidation in the left lower lobe (arrow) with surrounding ground-glass attenuation (halo sign), clustered centrilobular micronodules in the right lower lobe (circle), and a left pleural effusion (arrowheads).*

Case Presentation

A 68-year-old man recently underwent a renal transplantation procedure. His renal failure was attributed to immunosuppressive therapy from a liver transplant. Shortly after the renal transplant, he developed progressive respiratory distress and sepsis. Because the patient was immunocompromised, prophylactic therapy was started with antibiotic, antifungal, and antiviral drugs. Despite therapy, the patient's cardiopulmonary status continued to decline. CT of the chest was obtained to further investigate (**Figure 1**).

Differential Diagnosis

Post-transplant lymphoproliferative disorder
Septic emboli
Pulmonary cryptococcus
Invasive aspergillosis

Discussion

The risk of infectious syndromes in transplant recipients has traditionally been divided into three major time periods, each with varying probabilities of different microorganisms.[1] These time periods include the 1st month, 1st through 6th month, and 6th through 12th month post-transplantation. In the first month post-transplant, the major effects of exogenous immunosuppression are not yet apparent. As a result, the major causes of infection in the first month post-transplant are due to pre-existing infection from the donor or recipient and infectious complications from the transplant surgery itself or hospitalization. Microorganisms in this group include vancomycin-resistant enterococci, methicillin-resistant staphylococci, *Clostridium difficile*, and hepatitis B and C.[2]

Patients are most susceptible to the effects of immunosuppression in the first through sixth months post-transplant and, therefore, are at the greatest risk for opportunistic infections such as *Pneumocystis jirovecii*, cytomegalovirus, Epstein-Barr virus, and tuberculosis.[1] Although fungal infections such as histoplasmosis and cryptococcus most commonly occur during this period, they have been cited in the literature as being relatively uncommon unless the patient is receiving greater than normal amounts of immunosuppression, which was the case in this patient.[3,4]

From 6 to 12 months post-transplant, most patients have stable and reduced levels of immunosuppression. In this period, they are most susceptible to community-acquired pneumonias due to respiratory pathogens such as pneumococcus or legionella.[1]

Similar to other patients with prolonged hospitalizations and indwelling central venous catheters, transplant recipients are susceptible to pulmonary septic embolism, which may mimic the aforementioned infectious conditions. Organ transplant recipients are also susceptible to a large and varied group of lymphoproliferative diseases that occur after solid organ or stem cell transplantation, including lymphoid hyperplasias and malignancies, which may appear similar to infectious conditions on CT.

Post-Transplant Lymphoproliferative Disorder (PTLD)

PTLD is the second most common type of malignancy following transplantation and tends to occur at least one year following transplant.[5] Risk factors include primary Epstein-Barr infection, cytomegalovirus infection, and transplants from a seropositive donor to a seronegative donor. PTLD shares imaging characteristics of non-Hodgkin lymphoma and similarly has a variable manifestation depending on the organ involved. Although the abdomen is most commonly involved, pulmonary manifestations include pulmonary nodules and masses with homogenous soft-tissue attenuation on CT. The nodules and masses can have smooth or irregular borders. Although not typical of the condition, cases have demonstrated a ground-glass halo or central necrosis involving these lesions, mimicking the findings of pulmonary aspergillosis and septic pulmonary embolism.[6]

Septic Pulmonary Emboli

Pulmonary septic embolism is a condition in which infectious intravascular particles of thrombus containing microorganisms are embolized into the lungs via the pulmonary arterial system. Emboli may originate from many sources, but classically result from right-sided infective endocarditis from a mechanical valve or intravenous drug abuse. Infected deep venous thrombosis and infected catheters are additional potential sources. CT findings include multiple discrete nodules randomly distributed throughout the lungs that have a propensity to cavitate in various stages of evolution. Although ground-glass halos can form around the emboli, these are more typical of gram-negative septic emboli. Subpleural wedge-shaped consolidations are also a common feature secondary to infarction from occlusion of pulmonary arteries by septic emboli.[7]

Pulmonary Cryptococcosis

Pulmonary cryptococcosis is a form of pulmonary fungal infection most commonly caused by *Cryptococcus neoformans*. Typically, the respiratory tract is the primary route for entry of the fungal spores occurring via inhalation. The infection most commonly occurs in immunocompromised patients but has the potential to affect immunocompetent patients as well. The clinical presentation can range from asymptomatic nodular disease to severe acute respiratory distress syndrome. The most common CT findings are randomly distributed nodular or mass-like opacities. The opacities in pulmonary cryptococcus are typically smooth. In addition, peribronchovascular ground-glass opacities, mediastinal lymphadenopathy, and pleural effusions are common findings. Like several other entities, the smoothly marginated opacities can demonstrate the "halo sign" and create a diagnostic dilemma.[8]

Angioinvasive Aspergillosis

Angioinvasive aspergillosis is an infection caused by saprophytic airborne filamentous fungus Aspergillus species, usually *Aspergillus fumigatus*. It is the most severe and aggressive form of aspergillosis. It results from occlusion of small- to medium-sized pulmonary arteries by fungal hyphae. The most important risk factor is severe and prolonged neutropenia, almost always occurring in immunosuppressed patients. It is most commonly seen in graft-vs-host disease, in patients undergoing allogenic bone marrow transplantation and those with end-stage AIDS. CT findings include multiple pulmonary nodules and masses. The "halo sign" is classic for this condition and represents hemorrhage due to invasion of adjacent pulmonary vessels. Similar to septic emboli, peripheral wedge-shaped consolidations can be seen and represent hemorrhagic pulmonary infarction.[9]

Diagnosis

Pulmonary cryptococcosis

The left upper lobe consolidation was percutaneously sampled and returned positive for *Cryptococcus neoformans*. The patient's clinical symptoms improved, and imaging findings nearly completely resolved following antifungal therapy.

Summary

Despite improvements in immunosuppressive agents, infection remains a major barrier to disease-free survival following solid organ transplantation.[1] When a transplant recipient presents with an infectious syndrome, early and specific diagnosis and treatment are essential to optimize clinical outcomes. As cryptococcosis is most often associated with extrapulmonary findings such as meningitis, a negative work-up for these extrapulmonary findings can create a diagnostic dilemma for clinicians. As such, it is important for clinicians to be aware of the pulmonary findings of cryptococcosis along with the other conditions discussed.

References

1. Green M. Introduction: Infections in solid organ transplantation. Am J Transplant 2013;13(s4):3-8.
2. Mularoni A, Bertani A, Vizzini G, et al. Outcome of transplantation using organs from donors infected or colonized with carbapenem-resistant gram-negative bacteria. Am J Transplant 2015;15(10):2674-2682.
3. George I, Santos C, Powderly W, Olsen M. Epidemiology of cryptococcosis and cryptococcal meningitis in a large retrospective cohort of patients following solid organ transplantation. Open Forum Infect Dis 2017;4:1.
4. Karuthu S, Blumberg EA. Common infections in kidney transplant recipients. Clin J Am Soc Nephrol 2012;7(12):2058-2070.
5. Santos T, Aguiar B, Santos L, et al. Invasive fungal infections after kidney transplantation: a single-center experience. Transplant Proc 2015;47(4):971-975.
6. Camacho JC, Moreno CC, Harri PA, Aguirre DA, Torres WE, Mittal PK. Posttransplantation lymphoproliferative disease: proposed imaging classification. RadioGraphics 2014;34(7):2025-2038.
7. Borhani AA, Hosseinzadeh K, Almusa O, Furlan A, Nalesnik M. Imaging of posttransplantation lymphoproliferative disorder after solid organ transplantation. RadioGraphics 2009;29(4):981-1000.
8. Kwon WJ, Jeong YJ, Kim K-I, et al. Computed tomographic features of pulmonary septic emboli. J Comput Assist Tomogr 2007;31(3):390-394.
9. Song KD, Lee KS, Chung MP, et al. Pulmonary cryptococcosis: imaging findings in 23 non-AIDS patients. Korean J Radiol 2010;11(4):407-416.
10. Prasad A. Pulmonary aspergillosis: What CT can offer before it is too late! J Clin Diagnos Res 2016;10(4):TE01-TE05.

JAOCR at the Viewbox

David Radcliffe, M.D., Hemang Kotecha, D.O.

Department of Radiology, UMass Memorial Medical Center, Worcester, MA

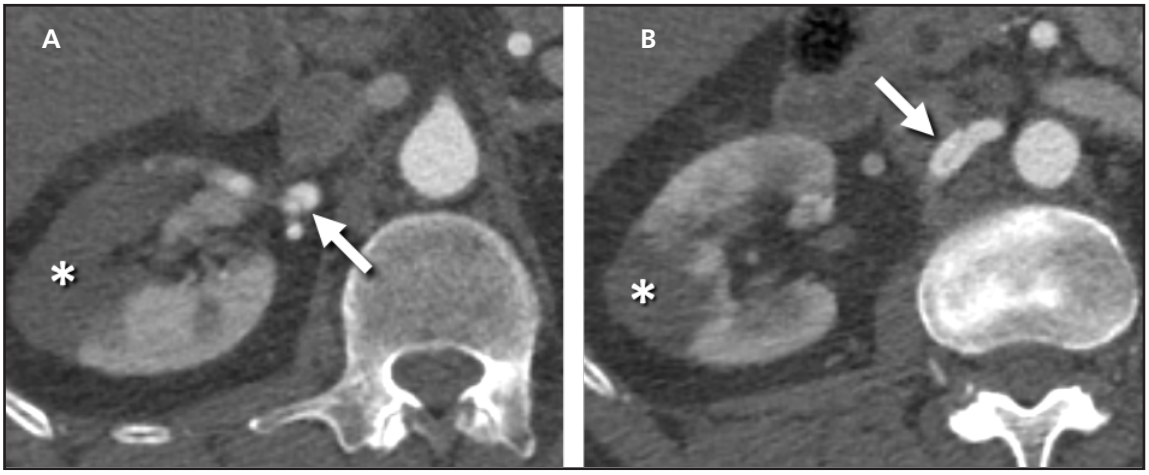

Spontaneous Renal Artery Dissection

A 55-year-old man with a 40 pack-year smoking history presented with acute onset right flank pain. A CT angiogram of the abdomen and pelvis was obtained following a renal abnormality seen on initial portal venous phase CT. Axial images of the right renal artery and kidney (**Figures A and B**) demonstrate a dissection flap (**arrows**), which begins approximately 3 cm from the ostium and extends into the inferior, lateral, and posterior branches. Approximately 20% of the right mid kidney is not perfused (**asterisks**).

Renal artery dissection is most often secondary to trauma, iatrogenic endovascular injury, or extension of an aortic dissection. Spontaneous renal artery dissection (SRAD) is described when there is no clear inciting event and is often associated with underlying arteriopathies, most notably fibromuscular dysplasia.[1,3] Diagnosis of SRAD often proves difficult due to the nonspecific clinical presentation, with flank pain and hematuria mimicking renal colic. The findings of SRAD are often imperceptible on ultrasound, the common first line imaging modality to evaluate such symptoms.[2] While angiography is considered the gold standard examination, CT or MR angiography remain the mainstay for noninvasive modalities to reliably establish timely and accurate diagnoses.[1,3]

Treatment of SRAD is dependent on several factors including extent of the vascular injury, stability of the dissection, and the patient's baseline and current renal function.[2] Goals of therapy are to preserve renal function and to treat renovascular hypertension. Treatment options include observation and medical management (antiplatelet, anticoagulation, and antihypertensive medications), endovascular stenting or coiling, surgical revascularization, and complete nephrectomy in severely damaged kidneys.[3]

References

1. Renaud S, Leray-Moragues H, Chenine L, et al. Spontaneous renal artery dissection with renal infarction. Clin Kidney J 2012;5(3):261-264.
2. Pellerin O, Garcon P, Beyssen B, et al. Spontaneous renal artery dissection: long-term outcomes after endovascular stent placement. J Vasc Interv Radiol 2009;20(8):1024-1030.
3. Kanofsky JA, Lepor H. Spontaneous renal artery dissection. Rev Urol 2007;9(3):156-160.

JAOCR at the Viewbox

Derek M. Chicarilli, M.D., M.A., Byron Chen, M.D.

Department of Radiology, UMass Memorial Medical Center, Worcester, MA

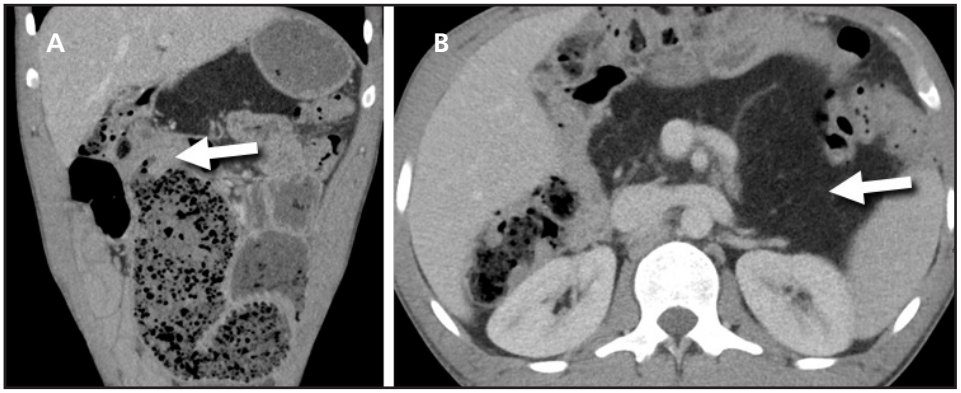

Distal Intestinal Obstruction Syndrome (DIOS)

A 35-year-old man presented to the emergency department with acute abdominal pain and he underwent intravenous contrast-enhanced CT of the abdomen and pelvis. Coronal CT image (**Figure A**) demonstrated an abrupt caliber transition (**arrow**) with dilated proximal small bowel containing bubbly fecalized material. Axial CT image (**Figure B**) at the level of the pancreas revealed complete fatty replacement and enlargment of the pancreas (**arrow**).

Cystic fibrosis is a relatively common inherited disease affecting multiple organ systems with increased thickness of mucous/secretions. The lungs, pancreas, and gastrointestinal (GI) tract are more commonly affected.[1,2] As treatments of pulmonary manifestations continually improve, familiarity with extrapulmonary adult manifestations is gaining importance with imagers.[1,2] A wide array of GI tract pathology has been described in cystic fibrosis patients including gastroesophageal reflux, DIOS, and constipation.[2]

In the cystic fibrosis patient population, DIOS occurs in up to 15% of the these patients.[1] It is characterized by the buildup of a mixture of viscous mucous and feculent material within the terminal ileum and/or right colon, leading to a bowel obstruction.[1,2] In cystic fibrosis patients, DIOS has been shown to more commonly occur in patients with pancreatic insufficiency, prior DIOS, a history of a meconium ileus episode, and dehydration.[1,2] Fatty replacement of the pancreas, as demonstrated in this case, is also commonly seen in cystic fibrosis and, although not specific, can be a tip-off to the interpreting radiologist to the presence of the disease.[1]

Imaging findings in DIOS include the findings of a small bowel obstruction including dilated loops of bowel proximal to the obstruction. At the transition point, there is a mass-like intraluminal soft-tissue density (representing the viscous secretions and fecal material) with internal gas bubbles. The images should also be critiqued for complications regarding the bowel obstruction, including perforation. Water-soluble contrast enema may be both diagnostic and therapeutic. Other treatment options include rehydration and stool softeners, with surgery reserved for complicated cases and/or cases that fail conservative treatment.[1]

References

1. Lavelle LP, McEvoy SH, Mhurchu EN, et al. Cystic fibrosis below the diaphragm: abdominal findings in adult patients. RadioGraphics 2015;35(3):680-695.

2. Morton J, Ansari N, Glanville A, Meagher AP, Lord RVN. Distal intestinal obstruction syndrome (DIOS) in patients with cystic fibrosis after lung transplantation. J Gastrointest Surg 2009;13:1448-1453.

JAOCR at the Viewbox

Tina Shiang, M.D., Christopher Cerniglia, D.O., M.Eng.

Department of Radiology, UMass Memorial Medical Center, Worcester, MA

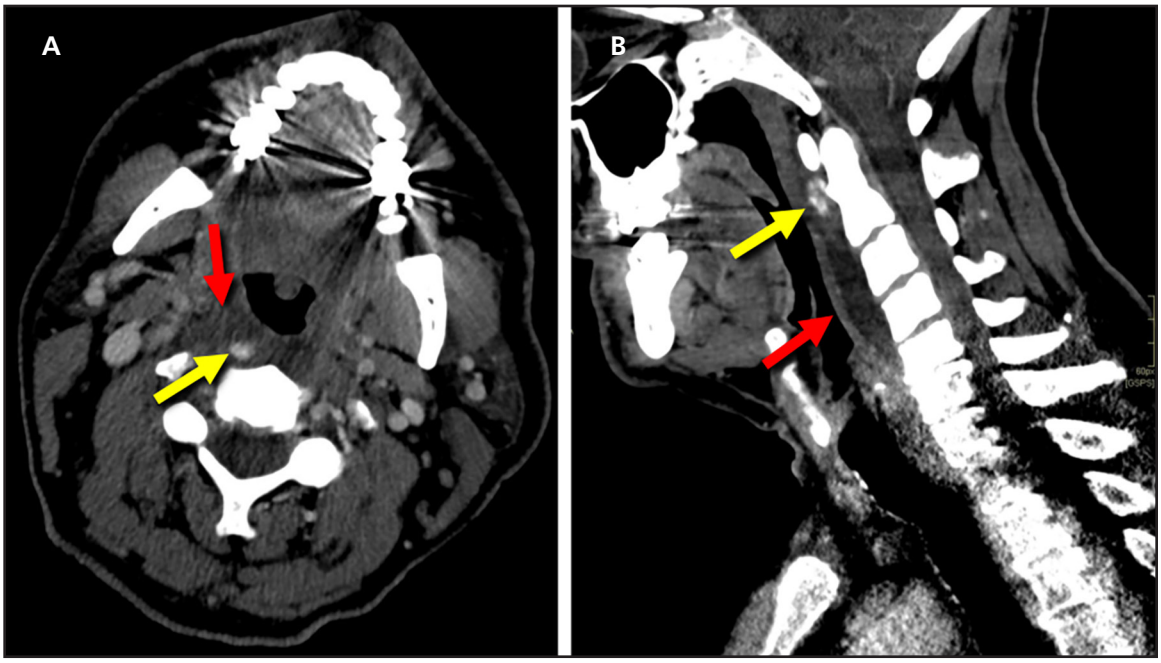

Calcific Tendinitis of the Longus Colli Muscle

A 50-year-old man presented with acute neck pain and limited range of motion. Axial (**Figure A**) and sagittal (**Figure B**) images from contrast-enhanced CT demonstrate an amorphous calcification in the prevertebral soft tissues at the level of the odontoid process (**yellow arrows**). A fusiform fluid collection measuring < 30 Hounsfield units smoothly enlarges the retropharyngeal space (**red arrows**) without rim enhancement or enhancing nodular component.

Calcific tendinitis of the longus colli muscle (also known as retropharyngeal tendinitis), is an acute inflammatory response to calcium hydroxyapatite crystal deposition in the longus colli muscle tendons.[1] Almost all patients present with neck pain and nearly half have swelling, limited range of motion, and odynophagia. Other frequent clinical findings may include low-grade fever and mildly elevated inflammatory markers.[1,2]

CT is the gold standard for diagnosis as it is most sensitive for detecting calcifications associated with this inflammatory process. These calcifications are typically within the prevertebral space at the C1-C2 level but can occur anywhere between C1-T3. Identifying calcification within this classic location is an important diagnostic feature to distinguish it from a potentially life-threatening retropharyngeal abscess, which presents as a rim-enhancing fluid collection, suppurative retropharyngeal adenopathy, and mass effect. The differential diagnosis also includes trauma, tumor, disc herniation, and epidural abscess.

Calcific tendinitis of the longus colli muscle is a self-limited process that resolves in 1 to 2 weeks and is treated conservatively with supportive care, NSAIDS, and corticosteroids.[1,2] No follow-up imaging is necessary.

References

1. Alamoudi U, Al-Sayed AA, AlSallumi Y, et al. Acute calcific tendinitis of the longus colli muscle masquerading as a retropharyngeal abscess: a case report and review of the literature. Int J Surg Case Rep 2017;41:343-346.
2. Park R, Halpert DE, Baer A, Holt PA. Retropharyngeal calcific tendinitis: case report and review of the literature. Semin Arthritis Rheum 2010;39:504-509.